5-1-2010

Quantum Electron Transport through Non-traditional Networks: Transmission Calculations using a Renormalization Group Method

Chris Varghese

QUANTUM ELECTRON TRANSPORT THROUGH NON-TRADITIONAL NETWORKS: TRANSMISSION CALCULATIONS USING A RENORMALIZATION GROUP METHOD

By

Chris Varghese

A Thesis
Submitted to the Faculty of
Mississippi State University
in Partial Fulfillment of the Requirements
for the Degree of Master of Science
in Physics
in the Department of Physics & Astronomy

Mississippi State, Mississippi

May 2010

QUANTUM ELECTRON TRANSPORT THROUGH NON-TRADITIONAL NETWORKS: TRANSMISSION CALCULATIONS USING A RENORMALIZATION GROUP METHOD

By

Chris Varghese

Approved:

Mark A. Novotny Professor of Physics (Major Professor)	R. Torsten Clay Associate Professor of Physics (Committee Member)
Seong-Gon Kim Associate Professor of Physics (Committee Member)	David L. Monts Professor of Physics (Graduate Coordinator)

Gary L. Myers
Dean of the College of Arts & Sciences

Name: Chris Varghese

Date of Degree: May 1, 2010

Institution: Mississippi State University

Major Field: Physics

Major Professor: Dr. Mark A. Novotny

Title of Study: QUANTUM ELECTRON TRANSPORT THROUGH NON-TRADITIONAL NETWORKS: TRANSMISSION CALCULATIONS USING A RENORMALIZATION GROUP METHOD

Pages in Study: 55

Candidate for Degree of Master of Science

A general exact matrix renormalization group method is developed for solving quantum transmission through networks. Using this method transmission of spinless electrons is calculated for a Hanoi network and a (newly introduced) fully connected Bethe lattice. Plots of the transmission and wavefunctions are obtained through application of the derived Renormalization Group recursion relations. The plots reveal band gaps (which has possible application in nano devices) in HN3 networks while no band gaps are observed in HN5 networks. With the fully connected Bethe lattice a drastic reduction in the transmission (in comparison to the normal Bethe lattice) is observed. This reduction can be found to be a purely quantum mechanical effect.

Key words: renormalization group, electron transport, Bethe lattice, Hanoi network

ACKNOWLEDGMENTS

I thank Dr. Mark A. Novotny for directing this research, Dr. Stefan Boettcher for helpful discussions, and my committee members for their comments on this thesis.

TABLE OF CONTENTS

LIST OF FIGURES

LIST OF SYMBOLS, ABBREVIATIONS, AND NOMENCLATURE

- **RG** Renormalization Group
- **FCBL** fully connected Bethe lattice
- **HN2** Hanoi network of degree 2
- **HN3** Hanoi network of degree 3
- **HN5** Hanoi network of average degree 5
- t transmission amplitude
- r reflection amplitude
- T transmission coefficient
- R reflection coefficient
- E energy
- Einstein summation convention is used in this list as well as in Appendix(A)
- Matrices are represented by capital letters in boldface font. e.g. $\mathbf{M}$
- Vectors are represented by small or capital letters in boldface font. e.g. $\mathbf{w}$
- The dimension of a particular vector or matrix can usually be identified from the context. In case the dimension is to be explicitly specified, it will appear as a subscript within braces. e.g. $\mathbf{M}_{[p]}$ represents a $p \times p$ square matrix; $\mathbf{M}_{[p,q]}$ represents a $p \times q$ matrix.
- The matrix $\mathbf{I}$ represents an identity matrix , i.e. $I_{ij} = \delta_{ij}$.
- The matrix $\mathbf{J}$ represents a matrix with all elements as unity, i.e. $J_{ij} = 1$.
- The vector $\mathbf{h}$ represents a vector with all elements as unity, i.e. $h_i = 1$
- A RG variable will have the RG step within brackets as a superscript. e.g. $\kappa^{(m)}$ represents the RG variable κ at the end m RG steps.
- When the RG step is not to be specified, the RG variable is used without any superscript. Then the RG variable after an RG step is represented with a prime. e.g. κ' represents κ after an RG step. In other words $\left[\kappa^{(m)}\right]' = \kappa^{(m+1)}$.

CHAPTER 1

INTRODUCTION

1.1 Particle and potential barrier

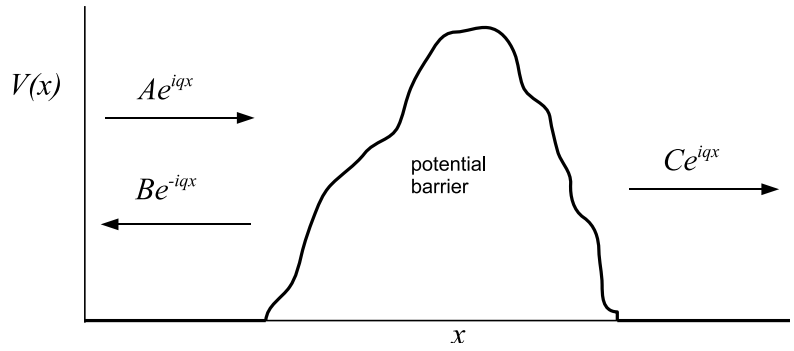

Figure 1.1

Particle incident on a 1-D potential barrier.

Consider a quantum particle of mass m and energy E incident from the left on a 1-D potential barrier $V(x)$ as shown in Fig. (1.1). In the steady state the particle's wavefunction $\psi(x)$ is given by the solution of the time independent Schrödinger equation

$$\mathcal{H}\psi(x) = \left(\frac{-\hbar^2}{2m}\frac{\mathrm{d}^2}{\mathrm{d}x^2} + V(x)\right)\psi(x) = E\psi(x). \tag{1.1}$$

The functional form of $\psi(x)$ on either side of the barrier is as shown in Fig. (1.1). The probability current is defined as [22]

$$j = \frac{\hbar}{2mi}\left(\psi^* \frac{\mathrm{d}\psi}{\mathrm{d}x} - \psi \frac{\mathrm{d}\psi^*}{\mathrm{d}x}\right). \tag{1.2}$$

The reflection and transmission amplitudes are

$$r = \frac{B}{A}; \qquad t = \frac{C}{A} \tag{1.3}$$

and the reflection and transmission coefficients are

$$R = \frac{j_{\text{reflected}}}{j_{\text{incident}}} = |r|^2; \qquad T = \frac{j_{\text{transmitted}}}{j_{\text{incident}}} = |t|^2 \tag{1.4}$$

with $R+T=1$. The probability that the incident particle is transmitted through (reflected from) the barrier and travels to $x=+\infty$ ($x=-\infty$) is T (R).

1.2 Matrix Equations for Transmission

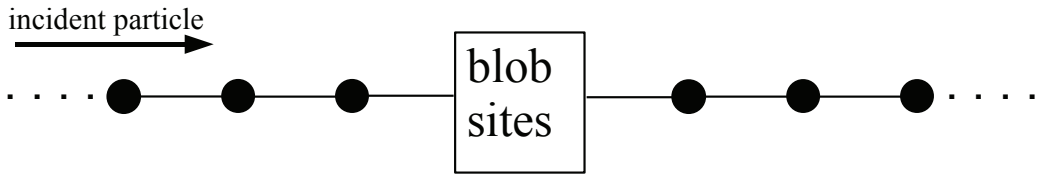

Figure 1.2

A blob connected to input and output leads.

Consider a nanoparticle consisting of a certain number of atoms. We call this nanoparticle a blob. The nanoparticle is connected to semi-infinite leads (chains of atoms separated

by a distance a) that form the input and output to the blob, as shown in Fig. (1.2). We are interested in calculating the transmission as a function of the energy, i.e. $T(E)$ through this blob for incident spinless electrons. The conductance G is related to T by the Landauer formula [20]. The calculation of T will require us to solve Equation (1.1). However the potential $V(x)$ is quite complicated and therefore an analytical solution is not possible.

Green's function [15] methods have been used extensively in the past to calculate the transmission [10, 16, 2, 29, 19, 13]. The Green's function is a very powerful concept and is especially useful when we try to include the effect of electron-electron or electron-phonon interactions [12]. However, we will restrict our study to non-interacting transport and therefore will resort to a much simpler formalism.

One approach to solve the quantum problem is to discretize Equation (1.1). In this process, the operators become matrices and functions become vectors. We label the input lead with negative integers and the output lead with positive integers. It can be found (see reference [14]) that for the Hamiltonian matrix, the diagonal elements $H_{ii} = V_{ii} + 2f = \epsilon_i$ = onsite energy of site i. A connection between site i and site j will produce an off-diagonal element $H_{ij} = -f =$ bond between i and j, with $f = \hbar^2/2ma^2$. All other elements of $\mathbf{H}$ are zero. This discretized Hamiltonian is equivalent to the tight-binding Hamiltonian [12].

Consequently we need to solve an infinite dimensional matrix equation

$$(H_{ij} - E\delta_{ij})\psi_j = 0. \tag{1.5}$$

For simplicity, we can set $\epsilon_i = 0, \quad f = 1$. Daboul et al. [11, 17] proposed the ansatz,

$$\psi_{-(m+1)} = e^{-imq} + re^{imq}; \qquad \psi_{(m+1)} = te^{imq}; \quad m \in \{0, 1, \ldots, \infty\} \tag{1.6}$$

which is valid for $q = \arccos(E/2)$. Using this, we can convert Equation (1.5) into a finite dimensional matrix equation

$$\begin{pmatrix} \xi & \mathbf{w}^{\mathrm{T}} & v \\ \mathbf{w} & \mathbf{A} & \mathbf{u} \\ v & \mathbf{u}^{\mathrm{T}} & \xi \end{pmatrix} \begin{pmatrix} 1+r \\ \psi \\ t \end{pmatrix} = \begin{pmatrix} 2i\Im(\xi) \\ 0 \\ 0 \end{pmatrix} \tag{1.7}$$

where $\xi = (-E + i\sqrt{4 - E^2})/2$ and matrix $\mathbf{A}$ is the blob Hamiltonian minus the energy. Vectors $\mathbf{w}$ and $\mathbf{u}$ correspond to the connections of the blob sites to the input and output respectively. The direct hopping between the input and the output lead is v.

1.3 Renormalization Group

The renormalization group (RG) is a mathematical technique that allows one to study the changes in a system as one views it at different distance scales. Consider a system consisting of a certain number of entities (e.g. atoms, electron spins, etc.) each of which have a "state variable" a_i associated with it. The entities interact with each other through a set of "coupling constants" b_{ij}. Suppose we have a function $Z(\{a_i\}, \{b_{ij}\})$ that describes the full physics of the system. Now suppose we are able to make a transformation [30]

$$\mathcal{R}(\{a_i\}, \{b_{ij}\}) = (\{a'_i\}, \{b'_{ij}\}) \tag{1.8}$$

such that

$$Z\left(\{a_i\}, \{b_{ij}\}\right) = Z\left(\{a'_i\}, \{b'_{ij}\}\right) \tag{1.9}$$

and

$$|\{a_i'\}| < |\{a_i\}| \tag{1.10}$$

then we say that this theory is renormalizable. The quantities $(\{a_i'\}, \{b_{ij}'\})$ are called renormalized quantities and seem to describe a system of smaller size but which nevertheless has the "same physics" as the original system. The transformation can be applied recursively to make the system size as small as required. So we can write Equation (1.8) in the form of a recursion relation

$$(\{a_i^{(m+1)}\}, \{b_{ij}^{(m+1)}\}) = \mathcal{R}(\{a_i^{(m)}\}, \{b_{ij}^{(m)}\}). \tag{1.11}$$

Here the integer m (initial system size $\geq m \geq$ final system size) labels the "RG step". Typically we run the recursion relations until we get a system with just one entity. The calculation of observables are significantly easier in the smaller system compared to the larger system and thus the RG has simplified the original problem. Additionally, the recursion relation Equation (1.11) can have fixed points. These fixed points will correspond to critical points of the system since critical points have the property that system has a behavior which is independent of the length scale [18].

One of the classic examples of RG is the block spin RG by Kadanoff [26]. Decimation RG within the Green's function formalism have been done in the past [3, 27]. In this thesis

we use an exact real space matrix RG to decimate the blob sites and thereby calculate t. In our case, the corresponding quantities in Equation (1.9) are

$$\{a_i\} \longrightarrow \text{onsite energies of the blob sites}$$

$$\{b_{ij}\} \longrightarrow \text{bonds between blob sites}$$

$$Z \longrightarrow \text{transmission coefficient}$$

CHAPTER 2

GENERAL MATRIX RG FORMULATION

Here we present a general real space decimation RG procedure that will be used in subsequent chapters. A related alternative decimation RG procedure involving Gaussian integrals was developed earlier that gives the same final RG equations [25].

2.1 Theory

Consider the blob in Equation (1.7) to be consisting of two sets (say X and Y) of sites. The matrix equation is

$$\begin{pmatrix} \xi_{\text{in}} & \mathbf{w}^{\mathrm{T}} & \mathbf{w_d}^{\mathrm{T}} & v \\ \mathbf{w} & \mathbf{A} & \mathbf{B} & \mathbf{u} \\ \mathbf{w_d} & \mathbf{B}^{\mathrm{T}} & \mathbf{D} & \mathbf{u_d} \\ v & \mathbf{u}^{\mathrm{T}} & \mathbf{u_d}^{\mathrm{T}} & \xi_{\text{out}} \end{pmatrix} \begin{pmatrix} 1+r \\ \boldsymbol{\psi} \\ \boldsymbol{\psi_d} \\ t \end{pmatrix} = \begin{pmatrix} 2i\Im(\xi) \\ 0 \\ 0 \\ 0 \end{pmatrix}. \tag{2.1}$$

Here $\mathbf{D}$ includes the interaction among all the sites in X, $\mathbf{A}$ includes the interaction among all the sites in Y, $\mathbf{B}$ includes the interaction of sites in X with those in Y. The vectors $\mathbf{w}$ and $\mathbf{u}$ includes connections between sites in X to the input and output respectively,

while $\mathbf{w_d}$ and $\mathbf{u_d}$ include the same for sites in Y. Notice that $\mathbf{D}$ and $\mathbf{A}$ are both symmetric matrices. Equation (2.1) represents four linear matrix equations which are

$$\xi_{\text{in}}(1+r) + \mathbf{w}^{\mathrm{T}}\boldsymbol{\psi} + \mathbf{w_d}^{\mathrm{T}}\boldsymbol{\psi_d} + vt = 2i\Im(\xi) \tag{2.2}$$

$$\mathbf{w}(1+r) + \mathbf{A}\boldsymbol{\psi} + \mathbf{B}\boldsymbol{\psi_d} + \mathbf{u}t = 0 \tag{2.3}$$

$$\mathbf{w_d}(1+r) + \mathbf{B}^{\mathrm{T}}\boldsymbol{\psi} + \mathbf{D}\boldsymbol{\psi_d} + \mathbf{u_d}t = 0 \tag{2.4}$$

$$v(1+r) + \mathbf{u}^{\mathrm{T}}\boldsymbol{\psi} + \mathbf{u_d}^{\mathrm{T}}\boldsymbol{\psi_d} + \xi_{\text{out}}t = 0. \tag{2.5}$$

Suppose we want to decimate all the sites in Y. We can solve Equation (2.4) for $\boldsymbol{\psi_d}$ to get

$$\boldsymbol{\psi_d} = -\mathbf{D}^{-1}[(1+r)\mathbf{w_d} + \mathbf{B}^{\mathrm{T}}\boldsymbol{\psi} + t\mathbf{u_d}]. \tag{2.6}$$

Substituting this in Equations (2.2), (2.3) and (2.5), we get

$$\xi_{\text{in}}(1+r) + \mathbf{w}^{\mathrm{T}}\boldsymbol{\psi} - \mathbf{w_d}^{\mathrm{T}}\mathbf{D}^{-1}[(1+r)\mathbf{w_d} + \mathbf{B}^{\mathrm{T}}\boldsymbol{\psi} + t\mathbf{u_d}] + vt = 2i\Im(\xi) \tag{2.7}$$

$$\mathbf{w}(1+r) + \mathbf{A}\boldsymbol{\psi} - \mathbf{B}\mathbf{D}^{-1}[(1+r)\mathbf{w_d} + \mathbf{B}^{\mathrm{T}}\boldsymbol{\psi} + t\mathbf{u_d}] + \mathbf{u}t = 0 \tag{2.8}$$

$$vt + \mathbf{u}^{\mathrm{T}}\boldsymbol{\psi} - \mathbf{u_d}^{\mathrm{T}}\mathbf{D}^{-1}[(1+r)\mathbf{w_d} + \mathbf{B}^{\mathrm{T}}\boldsymbol{\psi} + t\mathbf{u_d}] + \xi_{\text{out}}t = 0. \tag{2.9}$$

Equations (2.7), (2.8) and (2.9) can be written in the form of a matrix equation like Equation (2.1) as

$$\begin{pmatrix} \xi_{\text{in}} - \mathbf{w_d}^{\mathrm{T}}\mathbf{D}^{-1}\mathbf{w_d} & \mathbf{w}^{\mathrm{T}} - \mathbf{w_d}^{\mathrm{T}}\mathbf{D}^{-1}\mathbf{B}^{\mathrm{T}} & v - \mathbf{w_d}^{\mathrm{T}}\mathbf{D}^{-1}\mathbf{u_d} \\ \mathbf{w} - \mathbf{B}\mathbf{D}^{-1}\mathbf{w_d} & \mathbf{A} - \mathbf{B}\mathbf{D}^{-1}\mathbf{B}^{\mathrm{T}} & \mathbf{u} - \mathbf{B}\mathbf{D}^{-1}\mathbf{u_d} \\ v - \mathbf{u_d}^{\mathrm{T}}\mathbf{D}^{-1}\mathbf{w_d} & \mathbf{u}^{\mathrm{T}} - \mathbf{u_d}^{\mathrm{T}}\mathbf{D}^{-1}\mathbf{B}^{\mathrm{T}} & \xi_{\text{out}} - \mathbf{u_d}^{\mathrm{T}}\mathbf{D}^{-1}\mathbf{u_d} \end{pmatrix} \begin{pmatrix} 1+r \\ \boldsymbol{\psi} \\ t \end{pmatrix} = \begin{pmatrix} 2i\Im(\xi) \\ 0 \\ 0 \end{pmatrix}. \tag{2.10}$$

Thus we see that under the RG, the variables in Equation (2.1) transformed as

$$\begin{pmatrix} \xi_{\text{in}} \\ \xi_{\text{out}} \\ \mathbf{A} \\ \mathbf{w} \\ \mathbf{u} \\ v \end{pmatrix} \longrightarrow \begin{pmatrix} \xi_{\text{in}} - \mathbf{w_d}^{\mathrm{T}}\mathbf{D}^{-1}\mathbf{w_d} \\ \xi_{\text{out}} - \mathbf{u_d}^{\mathrm{T}}\mathbf{D}^{-1}\mathbf{u_d} \\ \mathbf{A} - \mathbf{B}\mathbf{D}^{-1}\mathbf{B}^{\mathrm{T}} \\ \mathbf{w} - \mathbf{B}\mathbf{D}^{-1}\mathbf{w_d} \\ \mathbf{u} - \mathbf{B}\mathbf{D}^{-1}\mathbf{u_d} \\ v - \mathbf{w_d}^{\mathrm{T}}\mathbf{D}^{-1}\mathbf{u_d} \end{pmatrix} = \begin{pmatrix} \xi'_{\text{in}} \\ \xi'_{\text{out}} \\ \mathbf{A}' \\ \mathbf{w}' \\ \mathbf{u}' \\ v' \end{pmatrix}. \tag{2.11}$$

For the networks that we study, $\mathbf{w_d} = 0$, $\mathbf{u_d} = 0$ and $v = 0$. This simplifies Equation (2.11) to

$$\mathbf{A} \longrightarrow \mathbf{A} - \mathbf{B}\mathbf{D}^{-1}\mathbf{B}^{\mathrm{T}} = \mathbf{A}'. \tag{2.12}$$

2.2 Some Examples

Here we apply the results obtained in the previous section to two simple networks. The RG shown for both the examples could also be achieved using decimation of a Green's function [28].

2.2.1 Linear Chain

Suppose we decimate the center site from a linear chain consisting of three sites, with the end sites attached to the input and output respectively [23]. Then for Equation (2.12) we have

$$\mathbf{A} = \begin{pmatrix} \kappa & 0 \\ 0 & \kappa \end{pmatrix} = \kappa\mathbf{I}; \qquad \mathbf{D} = \kappa\mathbf{I}; \qquad \mathbf{B} = \begin{pmatrix} \tau \\ \tau \end{pmatrix} = \tau\mathbf{h} \tag{2.13}$$

$$\Rightarrow \mathbf{A}' = \mathbf{A} - \mathbf{B}\mathbf{D}^{-1}\mathbf{B}^{\mathrm{T}} = \kappa\mathbf{I} - \tau\mathbf{h}\frac{1}{\kappa}\mathbf{I}\tau\mathbf{h}^{\mathrm{T}} \tag{2.14}$$

so that finally

$$\mathbf{A}' = \kappa\mathbf{I} - \frac{\tau^2}{\kappa}\mathbf{J} = \begin{pmatrix} \kappa - \tau^2/\kappa & -\tau^2/\kappa \\ -\tau^2/\kappa & \kappa - \tau^2/\kappa \end{pmatrix} = \begin{pmatrix} \kappa' & \tau' \\ \tau' & \kappa' \end{pmatrix}. \tag{2.15}$$

The RG equations for κ and τ contained in Equation (2.15) were first introduced by Aoki [3, 24].

2.2.2 Dangling Chain

Consider a blob consisting of a dangling chain of l sites as shown in Fig. (2.1). When we decimate the l-th site, for Equation (2.12) we have

$$\mathbf{A} = \kappa^{(0)}; \qquad \mathbf{D} = \kappa^{(0)}; \qquad \mathbf{B} = \tau \tag{2.16}$$

$$\Rightarrow \mathbf{A}' = \mathbf{A} - \mathbf{B}\mathbf{D}^{-1}\mathbf{B}^{\mathrm{T}} = \kappa^{(0)} - \frac{\tau^2}{\kappa^{(0)}} = \kappa^{(1)} \tag{2.17}$$

Now we decimate the $(l-1)$-th site. We have

$$\mathbf{A} = \kappa^{(0)}; \qquad \mathbf{D} = \kappa^{(1)}; \qquad \mathbf{B} = \tau \tag{2.18}$$

$$\Rightarrow \mathbf{A}' = \mathbf{A} - \mathbf{B}\mathbf{D}^{-1}\mathbf{B}^{\mathrm{T}} = \kappa^{(0)} - \frac{\tau^2}{\kappa^{(1)}} = \kappa^{(2)} \tag{2.19}$$

Thus, we find that the RG equation is

$$\kappa^{(m+1)} = \kappa^{(0)} - \frac{\tau^2}{\kappa^{(m)}}; \qquad 0 \leq m \leq l-1. \tag{2.20}$$

After decimating all the l sites in the chain, the blob is as shown in Fig. (2.1). In other words only a single site is left, with a renormalized on-site energy.

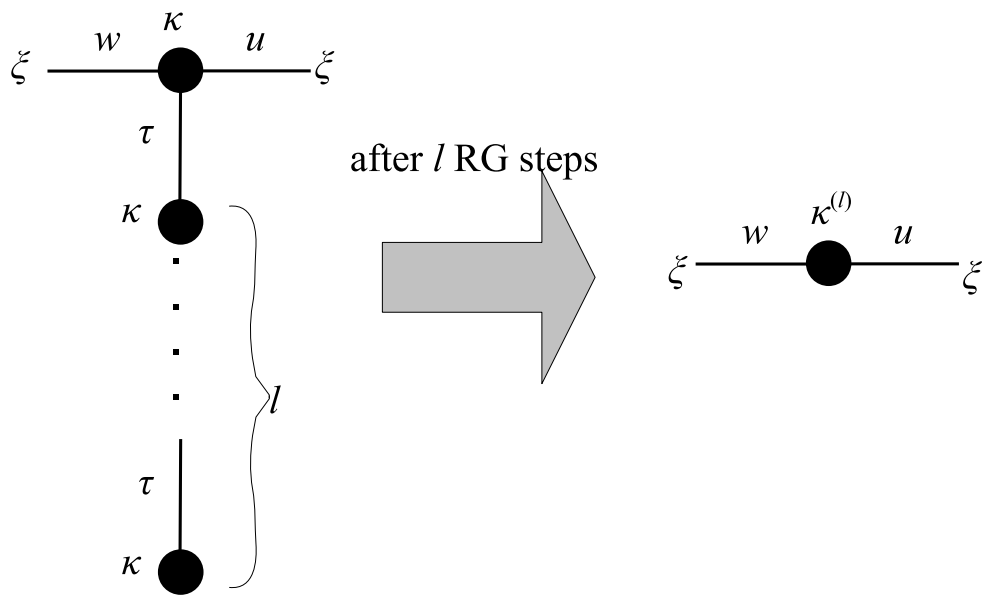

Figure 2.1

A dangling chain

CHAPTER 3

HANOI NETWORKS

Hanoi networks were introduced by Boettcher et al. [7, 8, 6]. Here we apply the results of the previous chapter to find the transmission through these networks.

3.1 Description of the Network

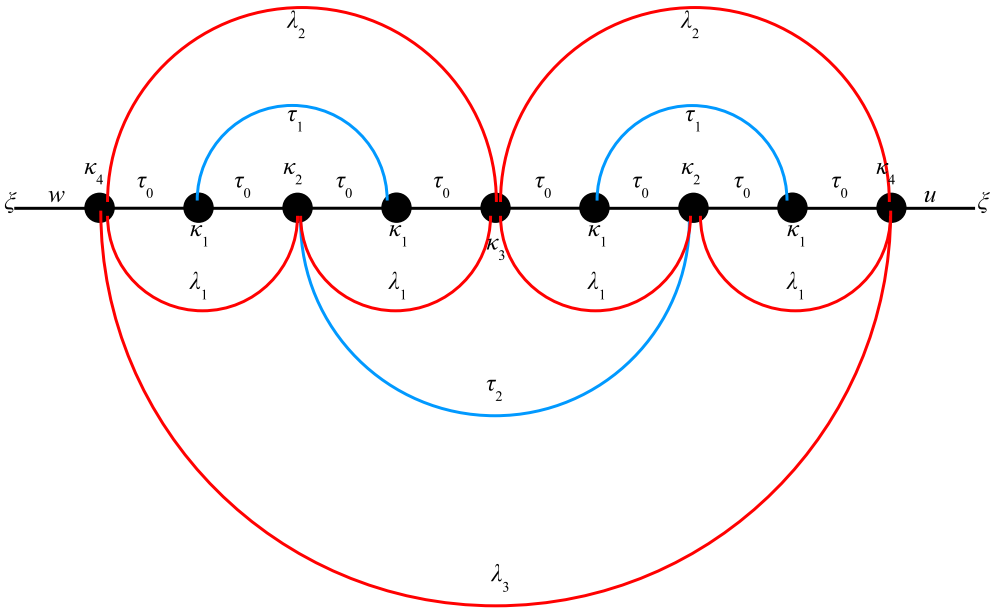

Figure 3.1

Linear hanoi network with $k = 3$.

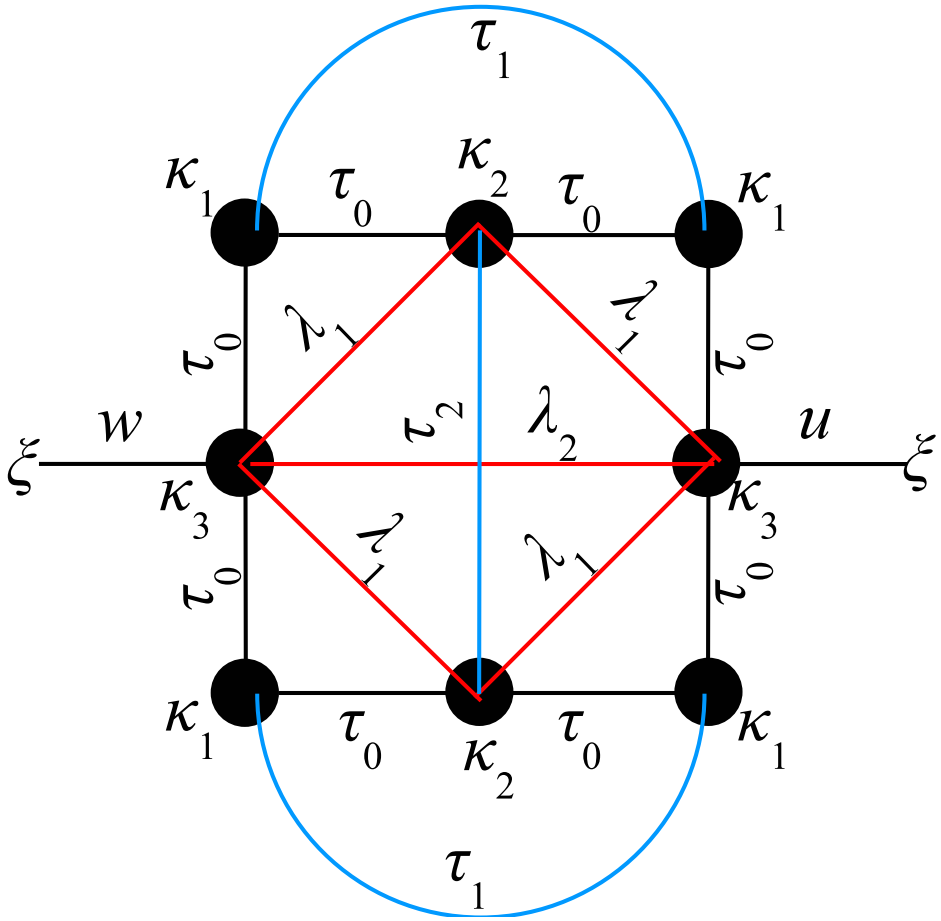

Figure 3.2

Ring hanoi network with $k = 3$

Hanoi networks have a nice hierarchical structure and come in two geometries – linear (Fig. (3.1)) and ring (Fig. (3.2)). It consists of a one dimensional backbone of N sites, where $N = 2^k + 1$ for the linear geometry and $N = 2^k$ for the ring geometry and k is a positive integer. The sites are labeled $0, 1, \ldots, N-1$. Any integer $n \in \{1, \ldots, N-1\}$ can be parameterized uniquely in terms of two other positive integers (i, j) as

$$n = 2^{i-1}(2j-1). \tag{3.1}$$

Each of the sites $1, \ldots, N-1$ can be labeled by (i, j) and thereby create a particular hierarchical network by connecting sites with the same i. Here the i represents the level in the hierarchy and j represents the index in a particular level. Considering the symmetry of the network, site 0 can be take to have parameters $(i = k+1, j = 0)$ in a linear geometry and $(i = k, j = 0)$ in a ring geometry. Notice that for a linear geometry when $i \in \{1, \ldots, k\}$; $\quad j \in \{1, \ldots, 2^{k-i}\}$ and when $i = k+1$; $\quad j \in \{0, 1\}$. Similarly for a ring geometry when $i \in \{1, \ldots, k-1\}$; $\quad j \in \{1, \ldots, 2^{k-i}\}$ and when $i = k$; $\quad j \in \{0, 1\}$.

Neighboring sites are connected by a bond of strength τ_0. Site 0 is connected to the input by w. In a linear geometry, site 2^k is connected to the output by u while in a ring geometry it is site 2^{k-1} that is connected to the output. Sites at level i have an onsite energy corresponding to κ_i. Sites in level i are connected to *one* of their immediate neighbors *in the same level* by a bond τ_i, i.e. in level $i = 1$ site 1 is connected to site 3, site 5 is connected to site 7 and so on. Additionally, even sites can be parameterized as $n_{\text{even}} = 2^p q$; $\quad p \in \{1, 2, \ldots\}$, $\quad q \in \{0, 1, \ldots\}$. An even site (p, q) is connected to even sites $(p, q \pm 1)$ by a bond λ_p. Thus the energy and hopping parameters that specify a hanoi network are $\{w, u, \kappa_1, \ldots, \kappa_{k+1}, \tau_0, \ldots, \tau_{k-1}, \lambda_1, \ldots, \lambda_k\}$ for a linear geometry and

$\{w, u, \kappa_1, \ldots, \kappa_k, \tau_0, \ldots, \tau_{k-1}, \lambda_1, \ldots, \lambda_{k-1}\}$ for a ring geometry. With $\lambda_p = 0$, the network has a degree of 3 and is therefore called a HN3 network. With $\lambda_p \neq 0$, the network has an average degree of 5 and is therefore called a HN5 network. The linear chain discussed in subsection(2.2.1) can be treated as a hanoi network with $\tau_{p>0} = 0 = \lambda_p$ resulting in a degree of 2 and is therefore called a HN2 network [7].

3.2 Matrix RG

At each RG step, we decimate all the odd sites. As the small world interaction among odd sites are one sided, we can divide the network into blocks containing 5 sites and decimate the odd sites block by block (see Equation (A.7)). Let us start with the first block which contain sites 0,1,2,3 and 4. This decimation process for a linear geometry is shown in Fig. (3.3). Thus, here (see Section[2.1]) we have

$$\mathbf{A} = \begin{pmatrix} \kappa_{k+1} & \lambda_1 & \lambda_2 \\ \lambda_1 & \kappa_2 & \lambda_1 \\ \lambda_2 & \lambda_1 & \kappa_3 \end{pmatrix} \tag{3.2}$$

$$\mathbf{D} = \begin{pmatrix} \kappa_1 & \tau_1 \\ \tau_1 & \kappa_1 \end{pmatrix}; \qquad \mathbf{B} = \begin{pmatrix} \tau_0 & 0 \\ \tau_0 & \tau_0 \\ 0 & \tau_0 \end{pmatrix} = \tau_0 \begin{pmatrix} 1 & 0 \\ 1 & 1 \\ 0 & 1 \end{pmatrix}. \tag{3.3}$$

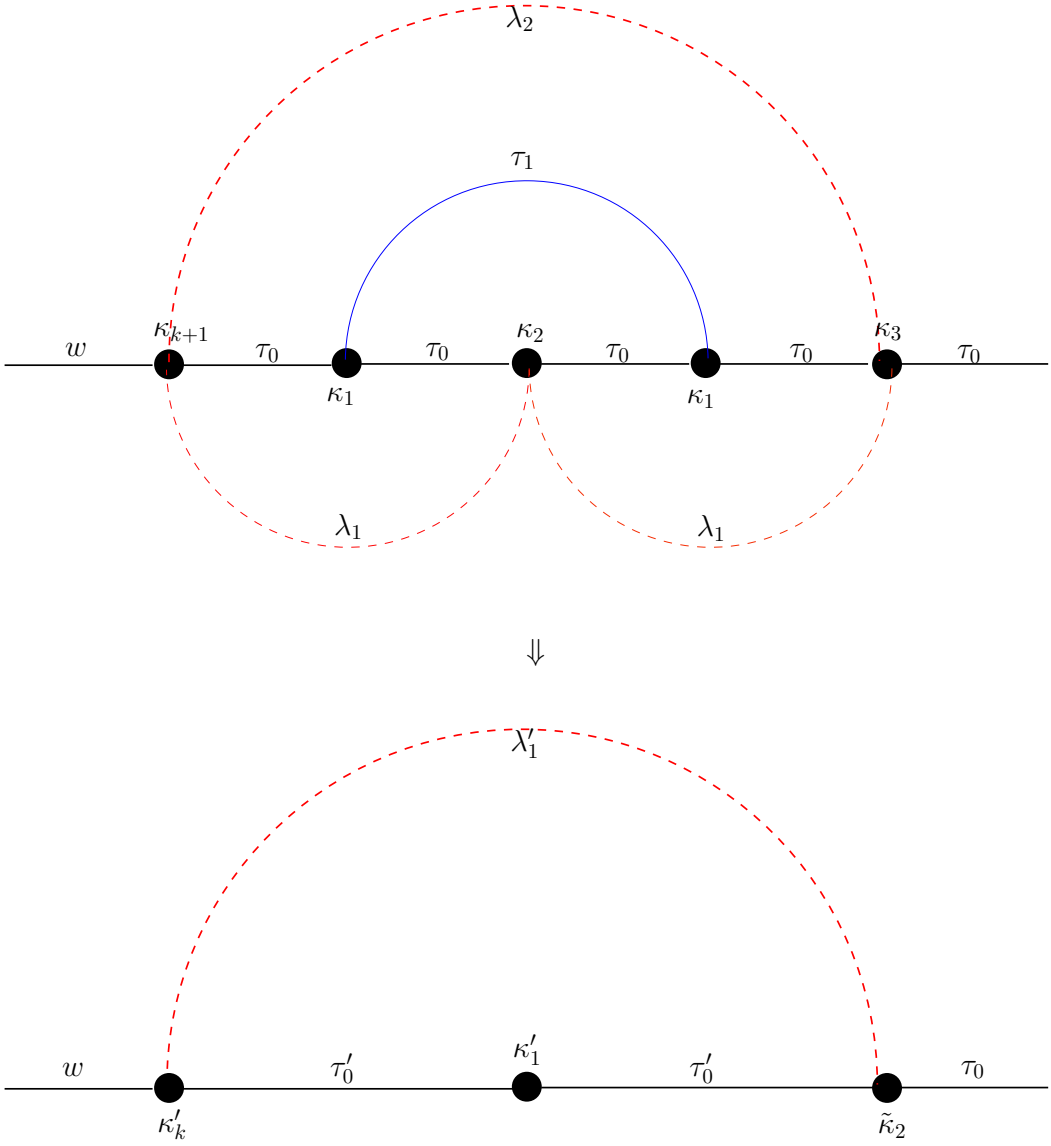

Figure 3.3

Decimation of a block

After decimation,

$$\mathbf{A}' = \begin{pmatrix} \kappa_k' & \tau_0' & \lambda_1' \\ \tau_0' & \kappa_1' & \tau_0' \\ \lambda_2 & \tau_0' & \tilde{\kappa}_2 \end{pmatrix} = \mathbf{A} - \mathbf{B}\mathbf{D}^{-1}\mathbf{B}^{\mathrm{T}} \tag{3.4}$$

$$= \begin{pmatrix} \kappa_{k+1} & \lambda_1 & \lambda_2 \\ \lambda_1 & \kappa_2 & \lambda_1 \\ \lambda_2 & \lambda_1 & \kappa_3 \end{pmatrix} - \tau_0^2 \begin{pmatrix} 1 & 0 \\ 1 & 1 \\ 0 & 1 \end{pmatrix} \frac{1}{\kappa_1^2 - \tau_1^2} \begin{pmatrix} \kappa_1 & -\tau_1 \\ -\tau_1 & \kappa_1 \end{pmatrix} \begin{pmatrix} 1 & 1 & 0 \\ 0 & 1 & 1 \end{pmatrix}. \tag{3.5}$$

After simplification, we find that

$$\kappa_k' = \kappa_{k+1} - \frac{\tau_0^2 \kappa_1}{\kappa_1^2 - \tau_1^2} \tag{3.6}$$

$$\kappa_1' = \kappa_2 - \frac{2\tau_0^2}{\kappa_1 + \tau_1} \tag{3.7}$$

$$\tilde{\kappa}_2 = \kappa_3 - \frac{\tau_0^2 \kappa_1}{\kappa_1^2 - \tau_1^2} \tag{3.8}$$

$$\tau_0' = \lambda_1 - \frac{\tau_0^2}{\kappa_1 + \tau_1} \tag{3.9}$$

$$\lambda_1' = \lambda_2 + \frac{\tau_0^2 \tau_1}{\kappa_1^2 - \tau_1^2}. \tag{3.10}$$

Here, the primed and unprimed quantities represent the 1-st and the 0-th level respectively in the RG recursion. Notice that the decimation of sites connected to site 4 is not complete yet and therefore its on-site energy will be modified further when we decimate the odd sites of the next block which contain sites 4,5,6,7 and 8.

After the decimation of the next block we get

$$\kappa_2' = \tilde{\kappa}_2 - \frac{\tau_0^2 \kappa_1}{\kappa_1^2 - \tau_1^2} = \kappa_3 - \frac{2\tau_0^2 \kappa_1}{\kappa_1^2 - \tau_1^2}. \tag{3.11}$$

Continuing the decimation block by block in this way, we find that

$$\kappa_i' = \kappa_{i+1} - \frac{2\tau_0^2\kappa_1}{\kappa_1^2 - \tau_1^2} \quad \text{for} \quad \forall i \in \{2, \ldots, k\} \tag{3.12}$$

$$\tau_i' = \tau_{i+1} \quad \forall i \geq 1 \tag{3.13}$$

$$\lambda_i' = \lambda_{i+1} \quad \forall i \geq 2. \tag{3.14}$$

At first it appears that there are a lot of RG variables to worry about. However most of these RG variables are interdependent. It can be deduced from Equations (3.6), (3.12), (3.13) and (3.14) that

$$\tau_1^{(m)} = \tau_{m+1} \tag{3.15}$$

$$\lambda_2^{(m)} = \lambda_{m+2}, \tag{3.16}$$

that the on-site energy parameter of the even sites is related to those of the odd sites as

$$\kappa_i^{(m)} = \kappa_1^{(m)} + \kappa_{m+i} - \kappa_{m+1} - 2(\lambda_1^{(m)} - \lambda_{m+1}) \quad \text{for} \quad \forall i \in \{2, \ldots, k-m\} \tag{3.17}$$

and that specifically for a linear geometry, the on-site energy parameter of the end sites

$$\kappa_{k+1-m}^{(m)} = \kappa_{k+1} + (\kappa_2^{(m)} - \kappa_{m+2})/2 \quad \text{for} \quad \forall m \in \{0, \ldots, k-2\}. \tag{3.18}$$

Thus we are left with just three independent RG variables which are $\kappa_1^{(m)}$, $\tau_0^{(m)}$ and $\lambda_1^{(m)}$ governed by the RG equations

$$\kappa_1^{(m+1)} = \kappa_1^{(m)} + \kappa_{m+2} - \kappa_{m+1} - 2(\lambda_1^{(m)} - \lambda_{m+1}) - \frac{2[\tau_0^{(m)}]^2}{\kappa_1^{(m)} + \tau_{m+1}} \quad \forall m \in \{0, \ldots, k-2\} \tag{3.19}$$

$$\tau_0^{(m+1)} = \lambda_1^{(m)} - \frac{[\tau_0^{(m)}]^2}{\kappa_1^{(m)} + \tau_{m+1}} \quad \forall m \in \{0, \ldots, k-1\} \tag{3.20}$$

$$\lambda_1^{(m+1)} = \lambda_{m+2} + \frac{[\tau_0^{(m)}]^2\tau_{m+1}}{[\kappa_1^{(m)}]^2 - \tau_{m+1}^2} \quad \forall m \in \{0, \ldots, k-1\}. \tag{3.21}$$

3.3 Calculation of Transmission and Wavefunctions

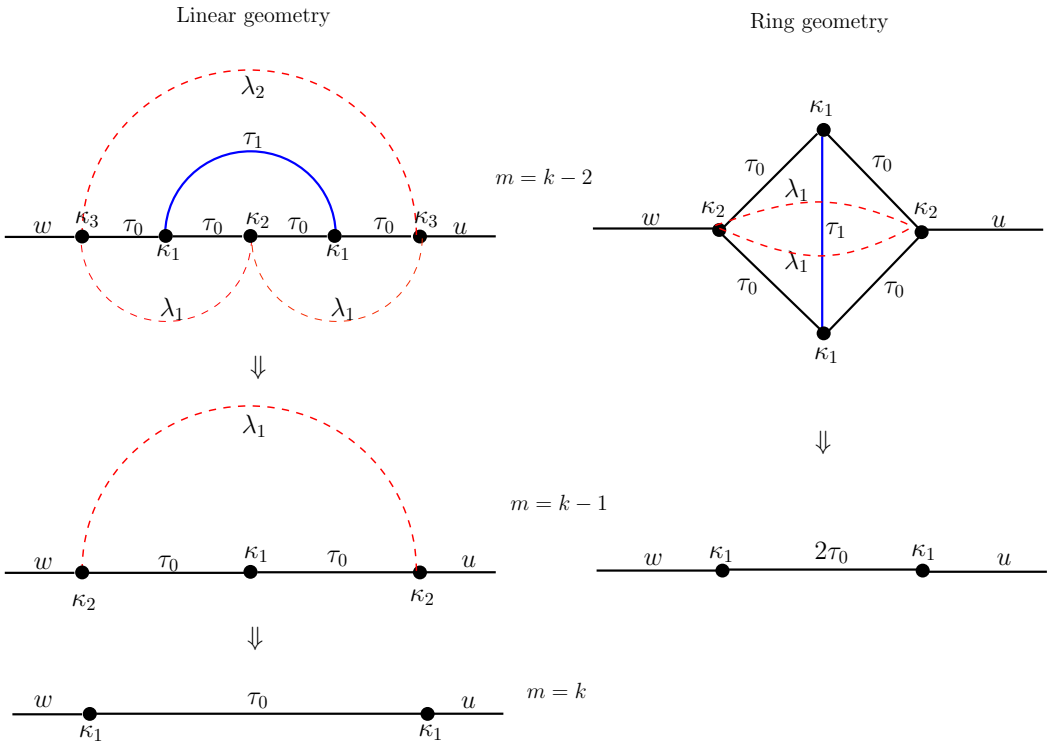

Figure 3.4

The last steps in the RG for the linear and ring geometry.

3.3.1 Linear geometry

Equations (3.17), (3.18), (3.19), (3.20), and (3.21) can be used to construct the $m = k - 2$ state shown in Fig. (3.4). The subsequent RG steps requires use of these equa-

tions with care. For the $m = k - 1$ RG step we proceed as follows. Using the RHS of Equation (3.17) with $i = 2$ we calculate

$$\tilde{\kappa}_2^{(k-1)} = \kappa_1^{(k-1)} + \kappa_{k+1} - \kappa_k - 2(\lambda_1^{(k-1)} - \lambda_k) \tag{3.22}$$

and then substitute $\kappa_2^{(k-1)}$ by $\tilde{\kappa}_2^{(k-1)}$ in the RHS of Equation (3.18) to get

$$\kappa_2^{(k-1)} = \kappa_{k+1} + \lambda_k - \lambda_1^{(k-1)} + \frac{1}{2}[\kappa_1^{(k-1)} - \kappa_k]. \tag{3.23}$$

This completes the $m = k - 1$ RG step. Now for $m = k$, we proceed in a similar way. Using the RHS of Equation (3.19) with $m = k - 1$ and $\tau_k = 0$, we calculate

$$\tilde{\kappa}_1^{(k)} = \kappa_1^{(k-1)} + \kappa_{k+1} - \kappa_k - 2(\lambda_1^{(k-1)} - \lambda_k) - \frac{2[\tau_0^{(k-1)}]^2}{\kappa_1^{(k-1)}} \tag{3.24}$$

and then with $m = k$, $i = 2$, $\lambda_{k+1} = 0$ and substituting $\kappa_1^{(k)}$ by $\tilde{\kappa}_1^{(k)}$ in the RHS of Equation (3.17), we calculate

$$\tilde{\kappa}_2^{(k)} = \tilde{\kappa}_1^{(k)} + \kappa_{k+2} - \kappa_{k+1} - 2\lambda_1^{(k)} \tag{3.25}$$

Substituting $m = k - 1$ in Equation (3.21) gives $\lambda_1^{(k)} = 0$. Finally, with $m = k$ and substituting $\kappa_2^{(k)}$ by $\tilde{\kappa}_2^{(k)}$ in the RHS of Equation (3.18), we get

$$\begin{aligned} \kappa_1^{(k)} &= \kappa_{k+1} + \lambda_k - \lambda_1^{(k-1)} - \frac{[\tau_0^{(k-1)}]^2}{\kappa_1^{(k-1)}} + \frac{1}{2}[\kappa_1^{(k-1)} - \kappa_k] \\ &= \kappa_{k+1} + \lambda_k + \tau_0^{(k)} - 2\lambda_1^{(k-1)} + \frac{1}{2}[\kappa_1^{(k-1)} - \kappa_k] \end{aligned} \tag{3.26}$$

After performing k RG steps, we are left with just $1 + 2^{k-k} = 2$ sites with an on-site energy corresponding to $\kappa_1^{(k)}$ and an interaction of $\tau_0^{(k)}$ between them. One site is

connected to the input by w while the other is connected to the output by u. In order to decimate these two sites, we have

$$\mathbf{A} = \begin{pmatrix} \xi & 0 \\ 0 & \xi \end{pmatrix}; \quad \mathbf{D} = \begin{pmatrix} \kappa_1^{(k)} & \tau_0^{(k)} \\ \tau_0^{(k)} & \kappa_1^{(k)} \end{pmatrix}; \quad \mathbf{B} = \begin{pmatrix} w & 0 \\ 0 & u \end{pmatrix} \tag{3.27}$$

$$\mathbf{A}' = \mathbf{A} - \mathbf{B}\mathbf{D}^{-1}\mathbf{B}^{\mathrm{T}} = \begin{pmatrix} \xi - \kappa_1^{(k)}\beta/\gamma & \beta\tau_0^{(k)} \\ \beta\tau_0^{(k)} & \xi - \kappa_1^{(k)}\beta\gamma \end{pmatrix} \tag{3.28}$$

where $\beta = wu/([\kappa_1^{(k)}]^2 - [\tau_0^{(k)}]^2)$, $\gamma = u/w$. Thus after decimating all $N = 1 + 2^k$ sites, we have

$$\begin{pmatrix} \xi - \kappa_1^{(k)}\beta/\gamma & \beta\tau_0^{(k)} \\ \beta\tau_0^{(k)} & \xi - \kappa_1^{(k)}\beta\gamma \end{pmatrix} \begin{pmatrix} 1+r \\ t \end{pmatrix} = \begin{pmatrix} 2i\Im(\xi) \\ 0 \end{pmatrix}. \tag{3.29}$$

From the above matrix equation,

$$\begin{pmatrix} 1+r \\ t \end{pmatrix} = \frac{2i\Im(\xi)}{(\xi - \kappa_1^{(k)}\beta/\gamma)(\xi - \kappa_1^{(k)}\beta\gamma) - \beta^2[\tau_0^{(k)}]^2} \begin{pmatrix} \xi - \kappa_1^{(k)}\beta\gamma \\ -\beta\tau_0^{(k)} \end{pmatrix}. \tag{3.30}$$

Thus we have found the transmission $T = |t|^2$.

Now using Equation (2.6) we can calculate the wavefunctions associated with the various sites. For simplicity we take $w = u$. To find the wavefunction associated with the highest level sites ($i = k + 1$), we start with the $m = k$ RG step given in Fig. (3.4). Here, for Equation (2.6), $\boldsymbol{\psi} = 0$, $\mathbf{w_d} = \begin{pmatrix} w \\ 0 \end{pmatrix}$, $\mathbf{u_d} = \begin{pmatrix} 0 \\ w \end{pmatrix}$ whereas the $\mathbf{D}$ and $\mathbf{B}$ matrices are given by Equation (3.2). Making these substitutions, we get

$$\boldsymbol{\psi}_{k+1} = \frac{-w}{[\kappa_1^{(k)}]^2 - [\tau_0^{(k)}]^2} \begin{pmatrix} (1+r)\kappa_1^{(k)} - t\tau_0^{(k)} \\ t\kappa_1^{(k)} - (1+r)\tau_0^{(k)} \end{pmatrix}. \tag{3.31}$$

Next we can find the wavefunction associated with the immediate lower level site($i = k$). Here, for Equation (2.6), $\boldsymbol{\psi} = \boldsymbol{\psi}_{k+1}$, $\mathbf{w_d} = 0 = \mathbf{u_d}$, $\mathbf{D} = \kappa_1^{(k-1)}$ and $\mathbf{B} = \tau_0^{(k-1)} \begin{pmatrix} 1 \\ 1 \end{pmatrix}$. Making these substitutions, we get

$$\boldsymbol{\psi}_k = \frac{\tau_0^{(k-1)} w(1+r+t)}{\kappa_1^{(k-1)}[\kappa_1^{(k)} + \tau_0^{(k)}]} \tag{3.32}$$

We can continue in this manner, in principle, to find the wavefunction of all the levels below. However the calculation gets very tedious and the expressions very complicated below $i = k$ and is therefore not given explicitly.

3.3.2 Ring geometry

We perform $k-1$ RG steps to be left with $2^{k-(k-1)} = 2$ sites. Site 1 is the nearest neighbor of site 0 and site 2=site 0 is the nearest neighbor of site 1. This makes the interaction between the two sites to be $2\tau_0^{(k-1)}$. The decimation of these two sites is similar to the case of the linear geometry, except that we need to replace $\kappa_1^{(k)}$ by $\kappa_1^{(k-1)}$ and $\tau_0^{(k)}$ by $2\tau_0^{(k-1)}$. So $\beta = wu/([\kappa_1^{(k-1)}]^2 - 4[\tau_0^{(k-1)}]^2)$ and

$$\begin{pmatrix} 1+r \\ t \end{pmatrix} = \frac{2i\Im(\xi)}{(\xi - \kappa_1^{(k-1)}\beta/\gamma)(\xi - \kappa_1^{(k-1)}\beta\gamma) - 4\beta^2[\tau_0^{(k-1)}]^2} \begin{pmatrix} \xi - \kappa_1^{(k-1)}\beta\gamma \\ -2\beta\tau_0^{(k-1)} \end{pmatrix}. \tag{3.33}$$

This completes the RG, giving the transmission $T = |t|^2$.

To find the wave functions here, we start at the $m = k-1$ RG step and proceed as we did in the case of the linear geometry. We find that,

$$\boldsymbol{\psi}_k = \frac{-w}{[\kappa_1^{(k-1)}]^2 - 4[\tau_0^{(k-1)}]^2} \begin{pmatrix} (1+r)\kappa_1^{(k-1)} - 2t\tau_0^{(k-1)} \\ t\kappa_1^{(k-1)} - 2(1+r)\tau_0^{(k-1)} \end{pmatrix} \tag{3.34}$$

and

$$\boldsymbol{\psi}_{k-1} = \frac{\tau_0^{(k-2)} w(1+r+t)}{[\kappa_1^{(k-2)} + \tau_1^{(k-2)}][\kappa_1^{(k-1)} + 2\tau_0^{(k-1)}]} \begin{pmatrix} 1 \\ \\ 1 \end{pmatrix}. \tag{3.35}$$

Notice that the two $i = k-1$ sites are symmetric. Therefore the wavefunctions obtained above for the two sites are identical as expected.

Again the wavefunction expressions for the lower i sites become complicated upon further iteration.

3.4 Transmission and Wavefunction plots

Using the results obtained in previous sections we can numerically plot the transmission. The *Mathematica* program given in Appendix (B) was used to obtain most of the plots in this section.

Fig. (3.5), Fig. (3.6) and Fig. (3.7) are plots of T *vs.* E for linear Hanoi networks with $\epsilon_i = 0$, $w = u = \tau_0 = -1$ and $k = 20$. Fig. (3.5) is for a HN2 network. Fig. (3.6) is for a HN3 network with $\tau_i = -1$. Fig. (3.7) is for a HN5 network with $\tau_i = \lambda_i = -1$.

As stated in Section (3.3), the RG does not simplify the calculation of wavefunctions of the Hanoi network. So for Fig. (3.8) and Fig. (3.9) the wavefunctions were calculated from the basic equation (and not by RG) for $k = 5$ and other parameters same as that for Fig. (3.6) and Fig. (3.7) respectively.

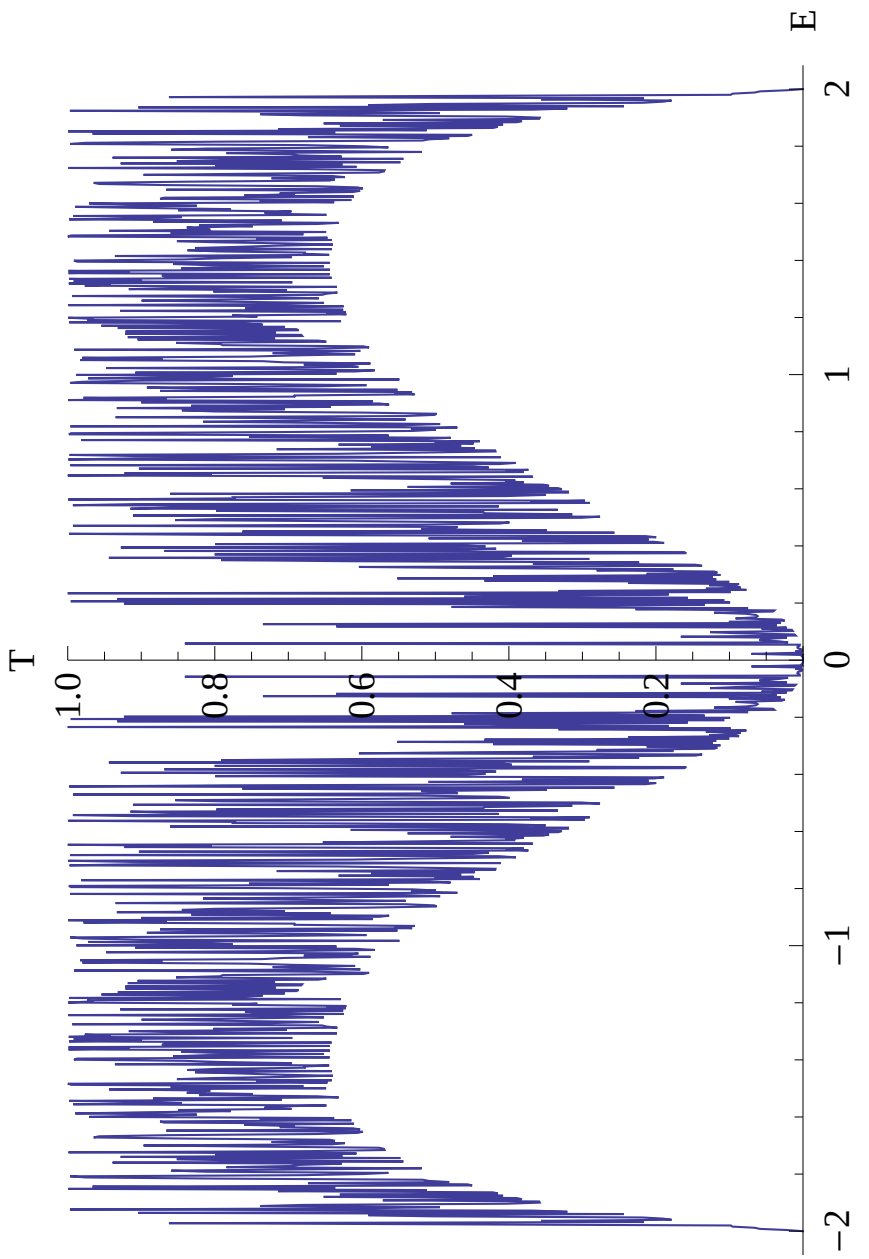

Figure 3.5

T *vs.* E for HN2.

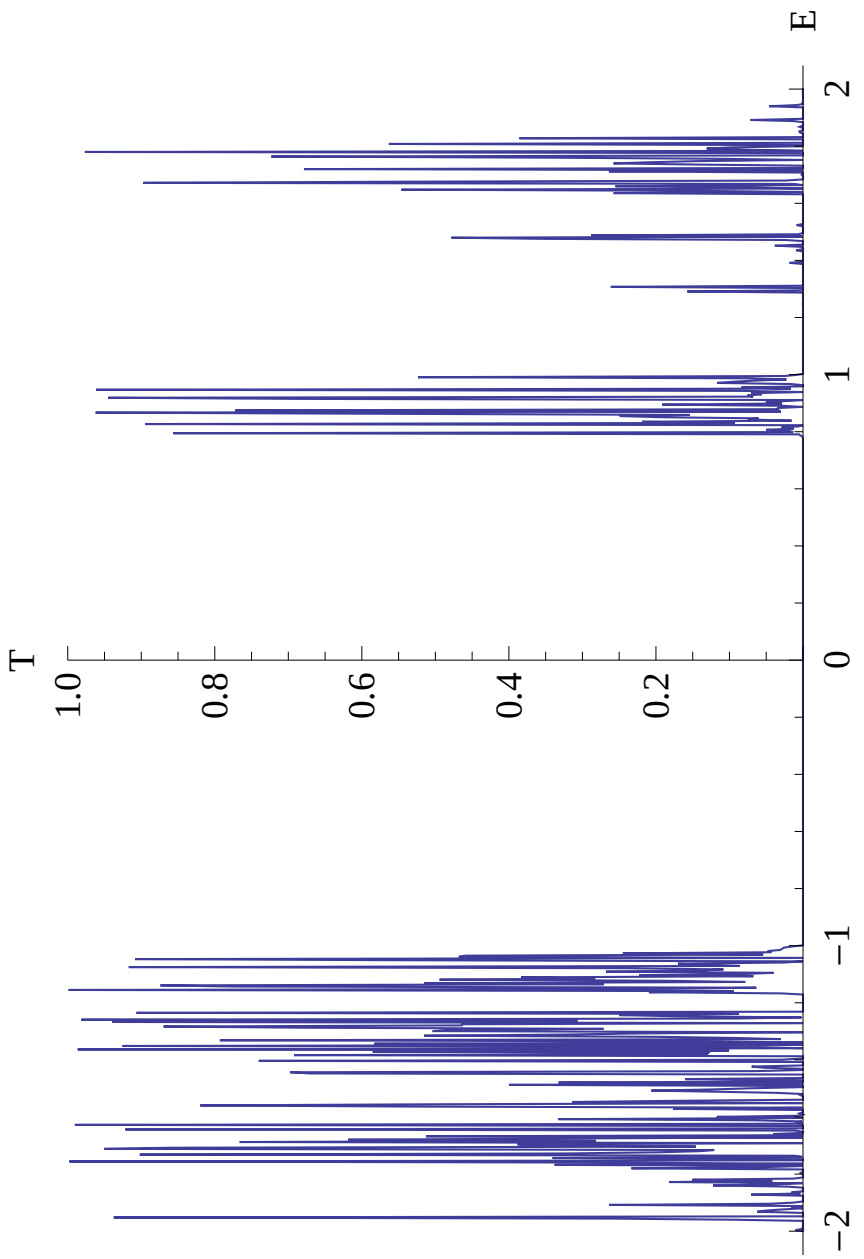

Figure 3.6

T *vs.* E for HN3.

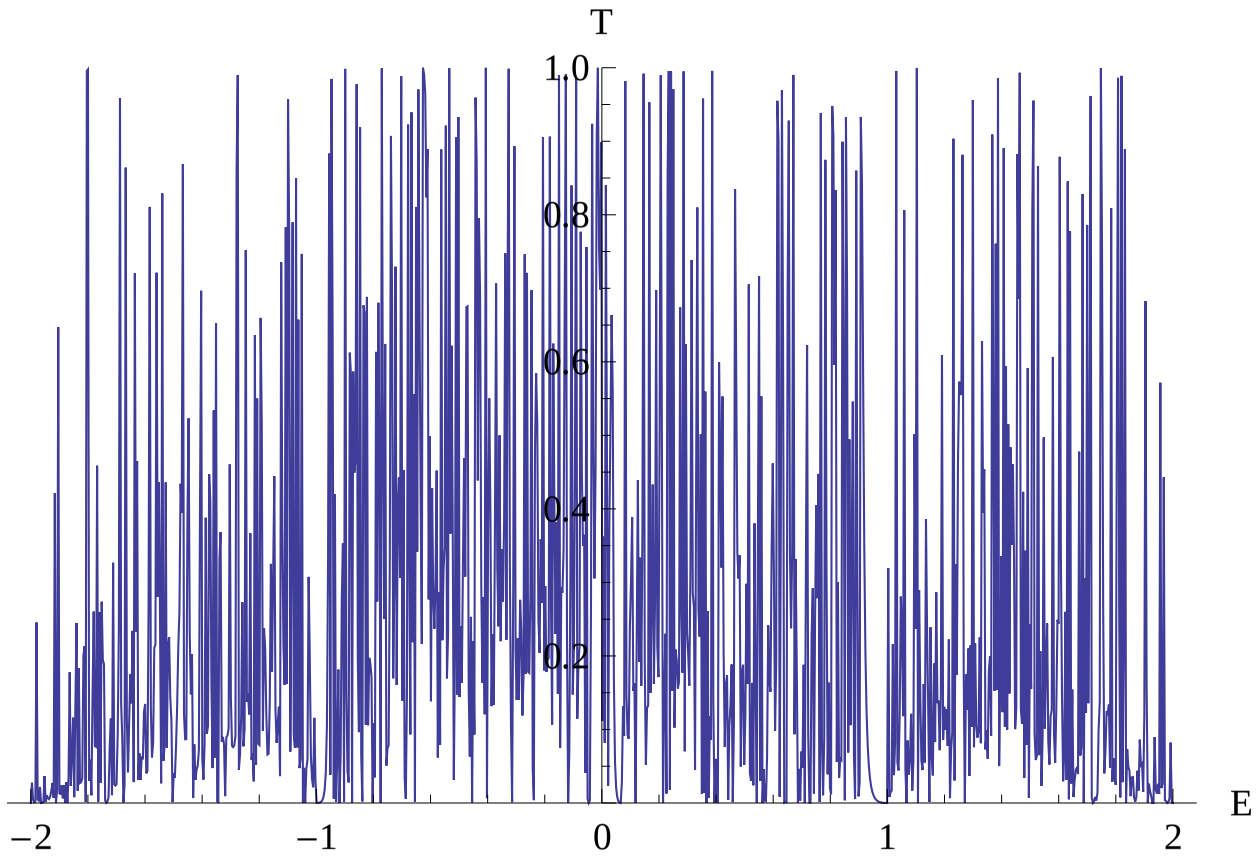

Figure 3.7

T vs. E for HN5.

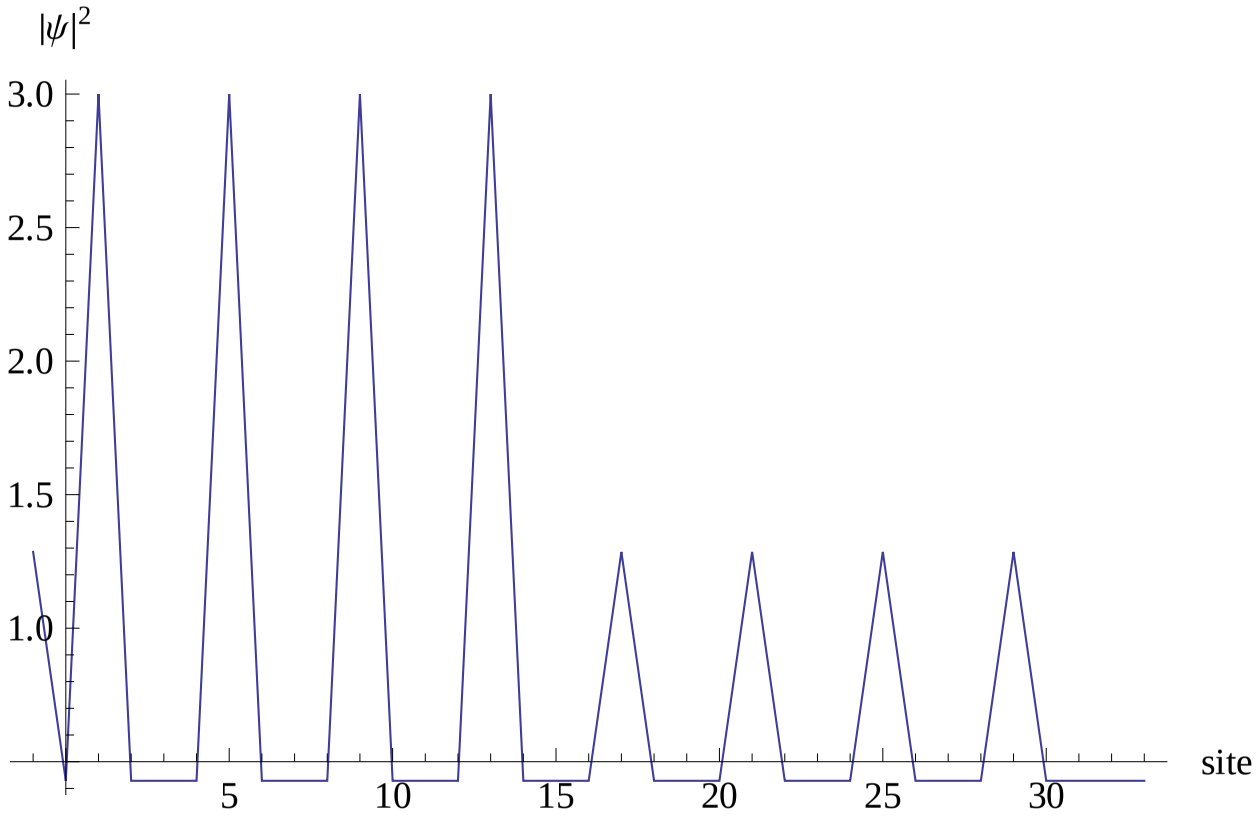

Figure 3.8

$|\psi|^2$ for HN3.

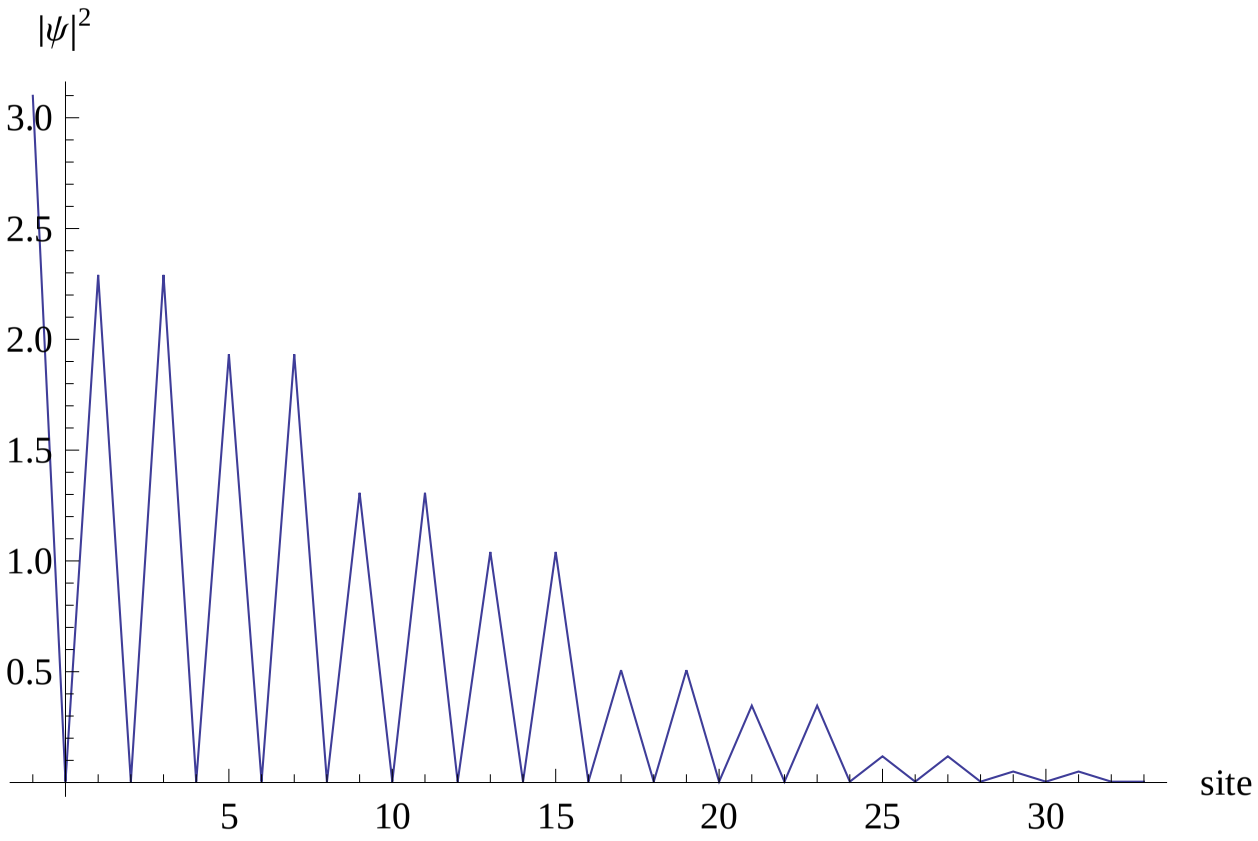

Figure 3.9

$|\psi|^2$ for HN5.

CHAPTER 4

FULLY CONNECTED BETHE LATTICE

The Bethe lattice was introduced by Hans Bethe [5]. Quantum transmission through a normal Bethe lattice has been studied in the past [21]. Here we study a more complicated variant of the Bethe lattice[1] which we call the fully connected Bethe lattice (FCBL).

4.1 Description of the Network

A normal Bethe lattice [1] as shown in Fig. (4.1) is characterized by two non-zero integers

$$k = \text{number of shells}$$

$$n = \text{number of branches coming out of a site}$$

Clearly the coordination number of every site is $n + 1$. The number of sites N_i in shell $i > 0$ can be found to be

$$N_i = (n + 1)n^{i-1}. \tag{4.1}$$

The variant of the Bethe lattice that we study has additional connections. All sites in a particular shell are fully connected among each other. Every site in the outermost

[1]Strictly speaking what we study is a finite Cayley tree. A Bethe lattice is the "deep" interior of an infinite Cayley tree, which makes all the sites in a Bethe lattice equivalent just as in a regular lattice [4]. However the terms Cayley tree and Bethe lattice are used interchangeably in the literature with the latter being more common in the physics community and therefore we stick with this term.

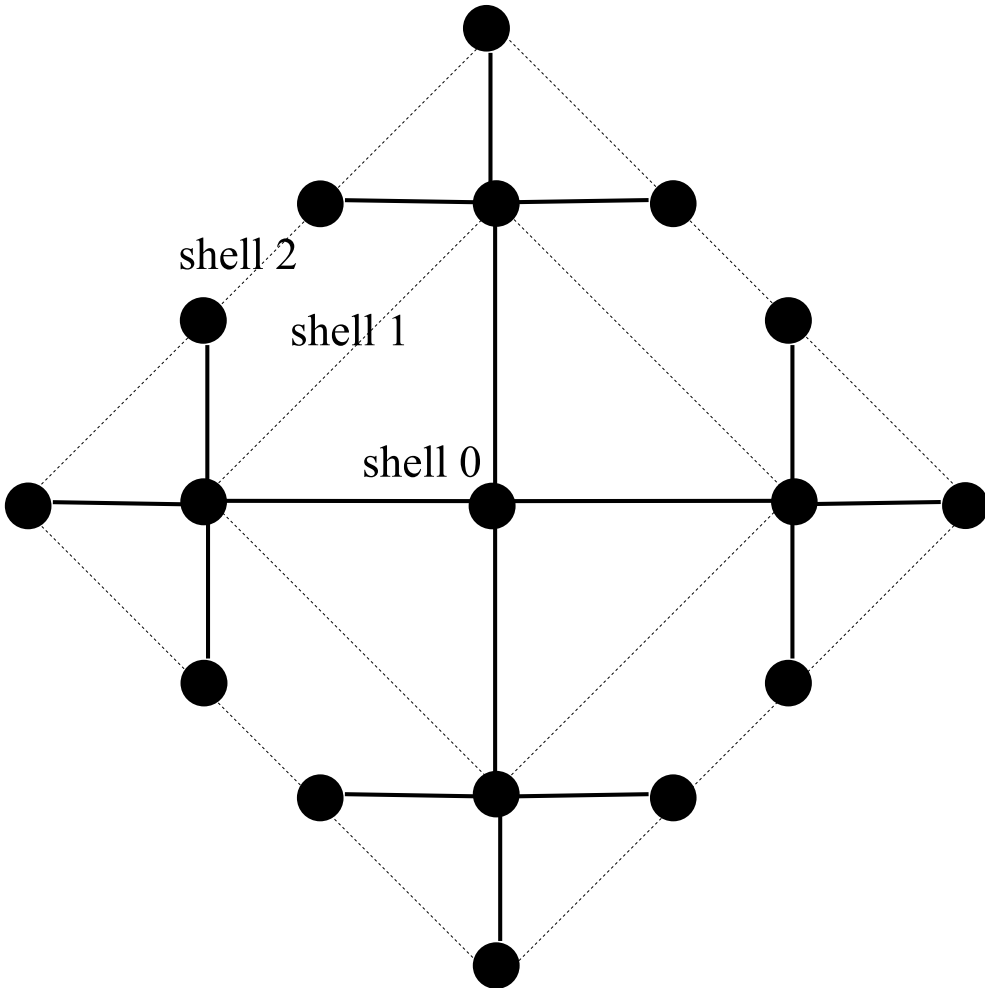

Figure 4.1

A normal Bethe lattice with $k = 2$ and $n = 3$.

shell is connected to the input while the zeroth shell site is connected to the output. The parameters of our FCBL are

$$\begin{aligned}
\kappa_i &= \text{onsite energy parameter of each site in the } i\text{-th shell} \\
s_i &= \text{connection between a site at the } i\text{-th shell and its root site} \\
\tau_i &= \text{connection between two sites in the } i\text{-th shell} \\
w &= \text{connection between each site in the } k\text{-th shell and the input} \\
u &= \text{connection between the zeroth shell site and the output.}
\end{aligned}$$

Thus, to specify a FCBL, the energy and hopping parameters to be specified are $\{w, u, \kappa_0, \ldots, \kappa_k, s_1, \ldots, s_k, \tau_1, \ldots, \tau_k\}$.

4.2 Matrix RG

We decimate the outermost shell at each RG step. Starting with the k-th shell, for Equation (2.12) we have (see List of Symbols, Abbreviations, and Nomenclature for definition of **I**, **J** and **h**)

$$\mathbf{D} = \begin{pmatrix} \kappa_k & \tau_k & \cdots & \tau_k \\ \tau_k & \kappa_k & & \vdots \\ \vdots & & \ddots & \tau_k \\ \tau_k & \cdots & \tau_k & \kappa_k \end{pmatrix} = (\kappa_k - \tau_k)\mathbf{I}_{[N_k]} + \tau_k \mathbf{J}_{[N_k]} \tag{4.2}$$

$$\mathbf{B} = \begin{pmatrix} s_k & \cdots & s_k & 0 & \cdots & \cdots & 0 \\ 0 & \cdots & 0 & \ddots & 0 & \cdots & 0 \\ 0 & \cdots & \cdots & 0 & s_k & \cdots & s_k \\ w & \cdots & \cdots & \cdots & \cdots & \cdots & w \end{pmatrix} = \begin{pmatrix} s_k \mathbf{I}_{[N_{k-1}]} \otimes \mathbf{h}_{[n]}^{\mathrm{T}} \\ w \mathbf{h}_{[N_k]}^{\mathrm{T}} \end{pmatrix} \tag{4.3}$$

$$\mathbf{A} = \begin{pmatrix} \kappa_{k-1} & \tau_{k-1} & \cdots & \tau_{k-1} & 0 \\ \tau_{k-1} & \kappa_{k-1} & & \vdots & \vdots \\ \vdots & & \ddots & \tau_{k-1} & \vdots \\ \tau_{k-1} & \cdots & \tau_{k-1} & \kappa_{k-1} & 0 \\ 0 & \cdots & \cdots & 0 & \xi \end{pmatrix} = \begin{pmatrix} (\kappa_{k-1} - \tau_{k-1})\mathbf{I}_{[N_{k-1}]} + \tau_{k-1}\mathbf{J}_{[N_{k-1}]} & 0 \\ 0 & \xi \end{pmatrix} \tag{4.4}$$

Using Equation (A.6) we get

$$\begin{aligned}
\mathbf{D}^{-1} &= \frac{1}{\kappa_k - \tau_k}\left(\mathbf{I}_{[N_k]} - \frac{\tau_k}{\kappa_k + (N_k-1)\tau_k}\mathbf{J}_{[N_k]}\right) = c(\mathbf{I}_{[N_k]} + d\mathbf{J}_{[N_k]}) \quad (4.5)\\
\Rightarrow \mathbf{D}^{-1}\mathbf{B}^{\mathrm{T}} &= c(\mathbf{I}_{[N_k]} + d\mathbf{J}_{[N_k]})\begin{pmatrix} s_k\mathbf{I}_{[N_{k-1}]} \otimes \mathbf{h}_{[n]} & w\mathbf{h}_{[N_k]}\end{pmatrix}\\
&= c\begin{pmatrix} s_k(\mathbf{I}_{[N_k]} + d\mathbf{J}_{[N_k]})(\mathbf{I}_{[N_{k-1}]} \otimes \mathbf{h}_{[n]}) & w(\mathbf{I}_{[N_k]} + d\mathbf{J}_{[N_k]})\mathbf{h}_{[N_k]}\end{pmatrix}\\
&= c\begin{pmatrix} s_k(\mathbf{I}_{[N_{k-1}]} \otimes \mathbf{h}_{[n]} + dn\mathbf{J}_{[N_k,N_{k-1}]}) & w(1+dN_k)\mathbf{h}_{[N_k]}\end{pmatrix}. \quad (4.6)
\end{aligned}$$

Simplifying $\mathbf{B}\mathbf{D}^{-1}\mathbf{B}^{\mathrm{T}}$ using Equations (A.5), (A.8), (A.9), (A.10) , and (A.11), and noting that $nN_{k-1} = N_k$, we get

$$\mathbf{B}\mathbf{D}^{-1}\mathbf{B}^{\mathrm{T}} = c\begin{pmatrix} ns_k^2(\mathbf{I}_{[N_{k-1}]} + nd\mathbf{J}_{[N_{k-1}]}) & ns_kw(1+dN_k)\mathbf{h}_{[N_{k-1}]}\\ ns_kw(1+dN_k)\mathbf{h}_{[N_{k-1}]}^{\mathrm{T}} & w^2N_k(1+dN_k)\end{pmatrix}. \quad (4.7)$$

Thus from Equation (2.12)

$$\mathbf{A}' = \begin{pmatrix} (\kappa_{k-1} - \tau_{k-1} - cns_k^2)\mathbf{I} + (\tau_{k-1} - cn^2s_k^2d)\mathbf{J} & -cns_kw(1+dN_k)\mathbf{h}\\ -cns_kw(1+dN_k)\mathbf{h}^{\mathrm{T}} & \xi - cw^2N_k(1+dN_k)\end{pmatrix}. \quad (4.8)$$

From Equation (4.8) we can identify the renormalized quantities as

$$\begin{aligned}
\kappa'_{k-1} &= \kappa_{k-1} - ns_k^2c(1+nd) \quad (4.9)\\
\tau'_{k-1} &= \tau_{k-1} - n^2s_k^2cd \quad (4.10)\\
w' &= -ns_kwc(1+N_kd) \quad (4.11)\\
\xi' &= \xi - N_kw^2c(1+N_kd). \quad (4.12)
\end{aligned}$$

Thus we have completed the decimation of the outermost shell. We can continue the decimation of the inner shells in this manner. After $m \in \{0, 1, \ldots, k-2\}$ RG steps, we find that

$$\kappa^{(m+1)} = \kappa_{k-m-1} - n s_{k-m}^2 c^{(m)}(1 + n d^{(m)}) \tag{4.13}$$

$$\tau^{(m+1)} = \tau_{k-m-1} - n^2 s_{k-m}^2 c^{(m)} d^{(m)} \tag{4.14}$$

$$w^{(m+1)} = -n s_{k-m} w^{(m)} c^{(m)}(1 + N_{k-m} d^{(m)}) \tag{4.15}$$

$$\xi^{(m+1)} = \xi^{(m)} - N_{k-m}[w^{(m)}]^2 c^{(m)}(1 + N_{k-m} d^{(m)}) \tag{4.16}$$

where we have used a simplified notation : $\kappa_{k-m}^{(m)} = \kappa^{(m)}$ and

$$c^{(m)} = \frac{1}{\kappa^{(m)} - \tau^{(m)}}; \qquad d^{(m)} = \frac{-\tau^{(m)}}{\kappa^{(m)} + (N_{k-m} - 1)\tau^{(m)}}. \tag{4.17}$$

For the last RG step i.e., $m = k - 1$ the n in Equations (4.13), (4.14), (4.15), and (4.16) should be replaced by $(n + 1)$ since the zeroth shell site has $n + 1$ branches coming out of it.

4.3 Calculation of Transmission and Wavefunctions

After performing k RG steps, we are left with just the zeroth shell site. To decimate this site, we have for Equation (2.12)

$$\mathbf{D} = \kappa^{(k)}; \qquad \mathbf{B} = \begin{pmatrix} w^{(k)} \\ \\ u \end{pmatrix}; \qquad \mathbf{A} = \begin{pmatrix} \xi^{(k)} & 0 \\ \\ 0 & \xi \end{pmatrix} \tag{4.18}$$

$$\Rightarrow \mathbf{A}' = \begin{pmatrix} \xi^{(k)} - \alpha/\delta & -\alpha \\ \\ -\alpha & \xi - \alpha\delta \end{pmatrix} \tag{4.19}$$

where $\alpha = w^{(k)}u/\kappa^{(k)}$ and $\delta = u/w^{(k)}$.

Thus after decimating all the sites, the equation to the solved is

$$\begin{pmatrix} \xi^{(k)} - \alpha/\delta & -\alpha \\ -\alpha & \xi - \alpha\delta \end{pmatrix} \begin{pmatrix} 1+r \\ t \end{pmatrix} = \begin{pmatrix} 2i\Im(\xi) \\ 0 \end{pmatrix}. \tag{4.20}$$

Solving, we get

$$\begin{pmatrix} 1+r \\ t \end{pmatrix} = \frac{2i\Im(\xi)}{\xi^{(k)}\kappa^{(k)}\xi - u^2\xi^{(k)} - [w^{(k)}]^2\xi} \begin{pmatrix} \kappa^{(k)}\xi - u^2 \\ w^{(k)}u \end{pmatrix}. \tag{4.21}$$

This completes the RG, giving the transmission $T = |t|^2$.

Due to the symmetry of the Bethe lattice, all sites at a particular shell have identical wavefunctions. We can use Equation (2.5) to calculate the wavefunction ψ_0 of the zeroth shell site. Here, for Equation (2.5), $v = 0$, $\boldsymbol{\psi} = 0$, $\mathbf{u_d}^{\mathrm{T}} = u$, $\xi_{\text{out}} = \xi$ and $\boldsymbol{\psi}_\mathbf{d} = \psi_0$. So we get

$$u\psi_0 + \xi t = 0 \Rightarrow \psi_0 = -\xi t/u. \tag{4.22}$$

For finding the wavefunctions of the sites in the outer shells, we can use Equation (2.2). At the $(k-i)-$th RG step for Equation (2.2), we have

$$\xi_{\text{in}} = \xi^{(k-i)}; \quad \mathbf{w}^{\mathrm{T}} = 0; \quad \mathbf{w_d}^{\mathrm{T}} = w^{(k-i)}\mathbf{h}_{[N_i]}^{\mathrm{T}}; \quad \boldsymbol{\psi}_\mathbf{d} = \psi_i\mathbf{h}_{[N_i]}; \quad v = 0. \tag{4.23}$$

Substituting in Equation (2.2), we get

$$\xi^{(k-i)}(1+r) + w^{(k-i)}\mathbf{h}_{[N_i]}^{\mathrm{T}}\psi_i\mathbf{h}_{[N_i]} = 2i\Im(\xi) \tag{4.24}$$

$$\Rightarrow \psi_i = \frac{2i\Im(\xi) - (1+r)\xi^{(k-i)}}{N_i w^{(k-i)}}. \tag{4.25}$$

4.4 Transmission and Wavefunction plots

Here we use the results from the previous section to numerically calculate and plot the transmission coefficient and the wavefunctions. The *Mathematica* programs given in Appendix (C) were used for getting the plots in this section.

All plots except Fig. (4.6) are for FCBLs with $k = 20$, $n = 2$, $\epsilon_i = 0$, $w = u = s_i = -1$. Fig. (4.7), Fig. (4.8), Fig. (4.9) and Fig. (4.10) are for energy $E = 1.5$.

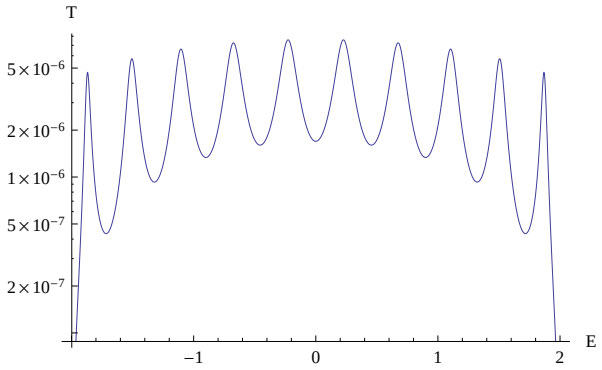

Figure 4.2

T *vs.* E for a normal Bethe lattice.

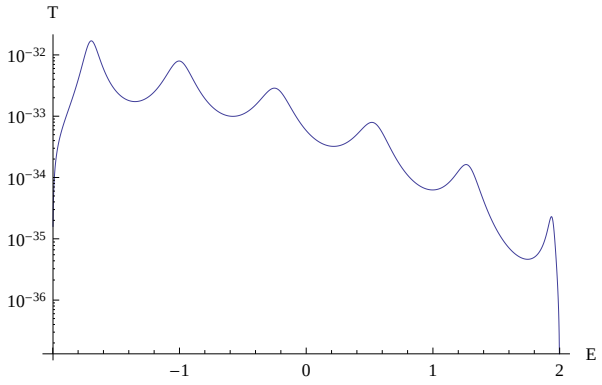

Figure 4.3

T *vs.* E for a FCBL with $\tau_i = -.001$.

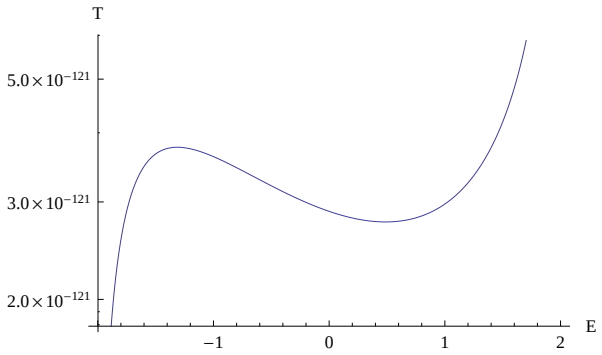

Figure 4.4

T *vs.* E for a FCBL with $\tau_i = -1$.

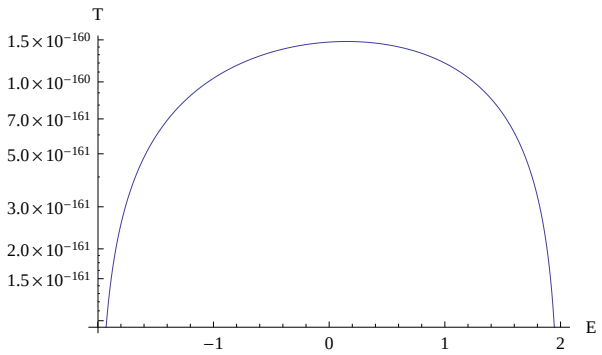

Figure 4.5

T *vs.* E for a FCBL with $\tau_i = -10$.

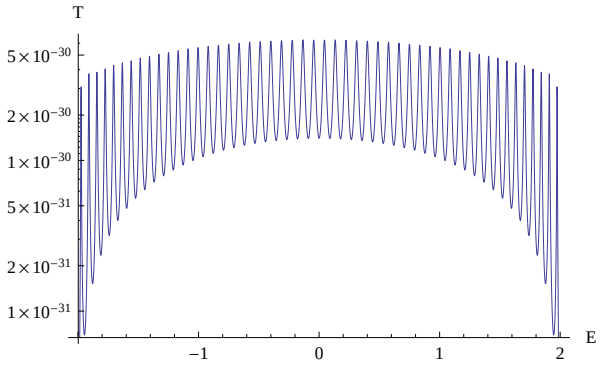

Figure 4.6

T *vs.* E for a normal Bethe lattice with $k = 100$.

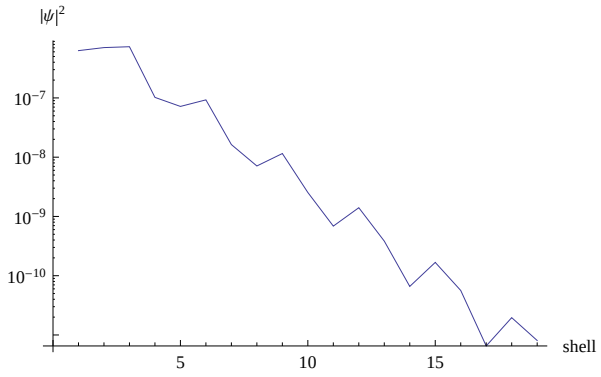

Figure 4.7

$|\psi|^2$ *vs.* shell number for a normal Bethe lattice.

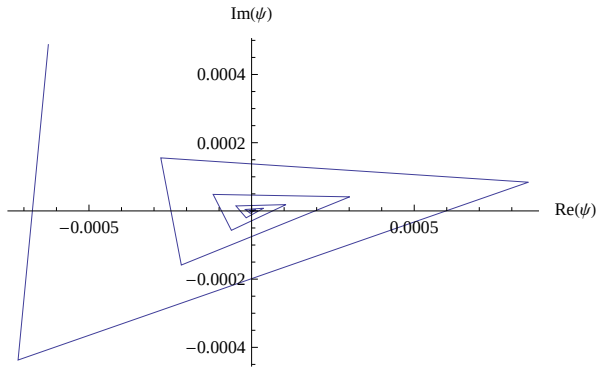

Figure 4.8

$\Im(\psi)$ *vs.* $\Re(\psi)$ for a normal Bethe lattice.

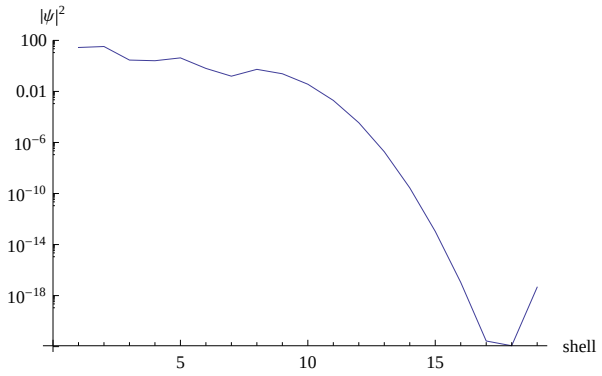

Figure 4.9

$|\psi|^2$ *vs.* shell number for a FCBL with $\tau_i = -.001$.

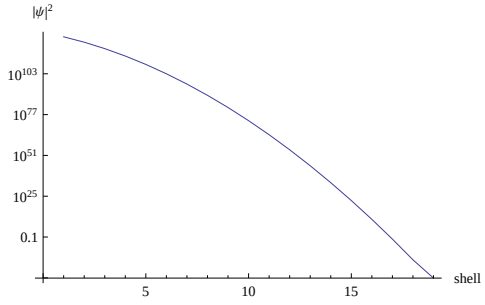

Figure 4.10

$|\psi|^2$ *vs.* shell number for a FCBL with $\tau_i = -10$.

CHAPTER 5

CONCLUSION AND DISCUSSION

The matrix RG developed in Section (2.1) is quite general and can be applied to any network provided they are renormalizable. An attempt at applying the matrix RG to a 2-D square lattice proved counter productive as many new interactions emerged in the renormalized lattice. However, only two-site interactions are ever present for our RG in contrast to most real-space RG procedures. For the two networks we studied, the renormalization group method significantly simplifies the calculation of the transmission probability and also wavefunctions in the case of the fully connected Bethe lattice. We have been able to study these networks of large size. With Hanoi networks, we have been able to find the transmission probability for $k = 200 \Rightarrow N = 2^{200} \approx 10^{60}$ sites. What is more interesting is that the RG is exact. While the work in this thesis has been limited to obtaining the RG equations and calculating the transmission probability, some striking observations from the numerical plots are worth mentioning.

Fig. (3.6) and Fig. (3.7) reveal a major difference between HN3 and HN5 networks — the presence of zero transmission regions (band gaps) in HN3 and their absence in HN5. The edges of these regions (band edges) correspond to a metal-insulator transition (MIT) of the nanoparticle. Such behavior is desirable for making non-linear nano-devices [27].

Further analysis of the RG equations can reveal and provide properties of these band edges [9].

The fully connected Bethe lattices in Fig. (4.2), Fig. (4.3), Fig. (4.4) and Fig. (4.5) differ only the value of τ_i. Since the τ bonds connect "equipotential" points, classically their presence should not produce any change in the transmission. However from these plots, we see that the transmission is reduced drastically as τ is increased. In the case of wavefunctions too, we notice a change in going from $\tau = 0$ to $\tau = -1$ as shown in figure Fig. (4.7) and Fig. (4.9). This is purely a quantum mechanical effect. Further analysis of the RG equations can help better understand this phenomenon [31].

Future work in this area could involve study of more complex networks, especially those that model real lattices. The creation of electronic devices at the nano scale by exploiting the band structure of these networks will be an exciting application of the study. Study of other processes like diffusion and phase transition on the networks would also be an interesting direction to proceed in.

REFERENCES

[1] R. Albert and A.-L. Barabási, "Statistical mechanics of complex networks," *Rev. Mod. Phys.*, vol. 74, no. 1, Jan 2002, pp. 47–97.

[2] R. F. S. Andrade and H. J. Schellnhuber, "Electronic states on a fractal: Exact Green's-function renormalization approach," *Phys. Rev. B*, vol. 44, no. 24, Dec 1991, pp. 13213–13227.

[3] H. Aoki, "Real-space renormalisation-group theory for Anderson localisation: decimation method for electron systems," *Journal of Physics C: Solid State Physics*, vol. 13, no. 18, 1980, p. 3369.

[4] R. J. Baxter, *Exactly solved models in statistical mechanics*, illustrated edition, Academic Press, 1982.

[5] H. A. Bethe, "Statistical Theory of Superlattices," *Proceedings of the Royal Society of London*, vol. 150, no. 871, July 1935, pp. 552–575.

[6] S. Boettcher and B. Gonalves, "Anomalous diffusion on the Hanoi networks," *EPL (Europhysics Letters)*, vol. 84, no. 3, 2008, 30002[6pp].

[7] S. Boettcher, B. Gonalves, and H. Guclu, "Hierarchical regular small-world networks," *J. Phys. A: Math. Theor.*, vol. 41, no. 25, 2008, 252001[7pp].

[8] S. Boettcher, B. Goncalves, and J. Azaret, "Geometry and dynamics for hierarchical regular networks," *Journal of Physics A: Mathematical and Theoretical*, vol. 41, no. 33, 2008, 335003[25pp].

[9] S. Boettcher, M. A. Novotny, and C. Varghese, "Quantum Transport through Hierarchical Structures," (to be submitted), 2010.

[10] S. Çalişkan, M. A. Novotny, and J. I. Cerdá, "Transport through small world networks," *Journal of Applied Physics*, vol. 102, no. 1, 2007.

[11] D. Daboul, I. Chang, and A. Aharony, "Series expansion study of quantum percolation on the square lattice," *Eur. Phys. J. B*, vol. 16, no. 2, 2000, pp. 303–316.

[12] S. Datta, *Electronic Transport in Mesoscopic Systems*, Cambridge University Press, 1997.

[13] S. Datta, "Nanoscale device modeling: the Green's function method," *Superlattices and Microstructures*, vol. 28, Oct. 2000, pp. 253–278.

[14] S. Datta, *Quantum Transport: Atom to Transistor*, 2nd edition, Cambridge University Press, 2005.

[15] D. K. Ferry and S. M. Goodnick, *Transport in Nanostructures*, Cambridge University Press, 2008.

[16] G. Grosso, S. Moroni, and G. P. Parravicini, "Recursion and Renormalization Methods in the Electronic Structure of Solids," *Physica Scripta*, vol. 1989, no. T25, 1989, p. 316.

[17] M. F. Islam and H. Nakanishi, "Localization-delocalization transition in a two-dimensional quantum percolation model," *Phys. Rev. E*, vol. 77, no. 6, 061109[9pp].

[18] L. P. Kadanoff, *Statistical physics: statics, dynamics and renormalization*, illustrated, reprint edition, World Scientific, 2000.

[19] Y.-J. Ko, M. Shin, J. S. Ha, and K. W. Park, "Green-Function Calculations of Coherent Electron Transport in a Gated Si Nanowire," *ETRI Journal*, vol. 22, no. 3, Sept. 2000, pp. 19–26.

[20] R. Landauer, "Spatial Variation of Currents and Fields Due to Localized Scatterers in Metallic Conduction," *IBM J. Res. Develop.*, vol. 1, no. 3, 1957, p. 223.

[21] Z. Lin and Y. Liu, "Electronic transport properties of the Bethe lattices," *Physics Letters A*, vol. 320, no. 1, 2003, pp. 70 – 80.

[22] E. Merzbacher, *Quantum Mechanics*, 3rd edition, Wiley, 1997.

[23] C. Monthus and T. Garel, "Anderson transitions: multifractal or non-multifractal statistics of the transmission as a function of the scattering geometry," *Journal of Statistical Mechanics: Theory and Experiment*, vol. 2009, no. 07, 2009, P07033[16pp].

[24] C. Monthus and T. Garel, "Statistics of renormalized on-site energies and renormalized hoppings for Anderson localization in two and three dimensions," *Phys. Rev. B*, vol. 80, no. 2, Jul 2009, 024203[11pp].

[25] M. A. Novotny, L. Solomon, C. Varghese, and S. Boettcher, "Renormalization Group Calculation of Electron Transport Through a Fully Connected Blob," *Physics Procedia*, 2010, (in press).

[26] R. K. Pathria, *Statistical Mechanics*, Butterworth-Heinemann, 1996.

[27] V. Pouthier and C. Girardet, "Electronic transmission through a metallic cluster attached to an adsorbed nanowire: creation of a nanoscale electronic on/off switch," *Surface Science*, vol. 511, no. 1, June 2002, pp. 203–214.

[28] V. Pouthier and C. Girardet, "Electronic transmission through a set of metallic clusters randomly attached to an adsorbed nanowire: Localization-delocalization transition," *Phys. Rev. B*, vol. 66, no. 11, Sep 2002, 115322[13pp].

[29] D. A. Ryndyk, R. Gutiérrez, B. Song, and G. Cuniberti, "Green Function Techniques in the Treatment of Quantum Transport at the Molecular Scale," *Springer Verlag Springer Series on Chemical Physics*, vol. 93, 2009, pp. 213–+.

[30] E. H. Stanley, "Scaling, universality, and renormalization: Three pillars of modern critical phenomena," *Rev. Mod. Phys.*, vol. 71, no. 2, Mar 1999, pp. S358–S366.

[31] C. Varghese and M. A. Novotny, "Quantum Transport through a Fully Connected Bethe Lattice," (to be submitted), 2010.

APPENDIX A

SOME MATRIX IDENTITIES

- A few basic identities:

$$\mathbf{h}\mathbf{h}^{\mathrm{T}} = h_i h_j = J_{ij} = \mathbf{J} \tag{A.1}$$

$$\mathbf{h}_{[p]}^{\mathrm{T}}\mathbf{h}_{[p]} = h_i h_i = p \tag{A.2}$$

$$\mathbf{J}_{[p]}\mathbf{J}_{[p]} = \mathbf{h}_{[p]}\mathbf{h}_{[p]}^{\mathrm{T}}\mathbf{h}_{[p]}\mathbf{h}_{[p]}^{\mathrm{T}} = \mathbf{h}_{[p]}p\mathbf{h}_{[p]}^{\mathrm{T}} = p\mathbf{h}_{[p]}\mathbf{h}_{[p]}^{\mathrm{T}} = p\mathbf{J}_{[p]} \tag{A.3}$$

$$\mathbf{J}_{[p]}\mathbf{h}_{[p]} = J_{ij}h_j = h_i h_j h_j = h_i p = p\mathbf{h} \tag{A.4}$$

$$\mathbf{h}_{[p]}^{\mathrm{T}}\mathbf{J}_{[p,q]} = p\mathbf{h}_{[q]}^{\mathrm{T}} \tag{A.5}$$

- Inverse of a matrix of the form $(a\mathbf{I} + b\mathbf{J})$
  Let $(a\mathbf{I} + b\mathbf{J})^{-1} = p\mathbf{I} + q\mathbf{J}$

$$\begin{aligned}
\Rightarrow (a\mathbf{I} + b\mathbf{J})(p\mathbf{I} + q\mathbf{J}) &= \mathbf{I} \\
\Rightarrow ap\mathbf{I}\mathbf{I} + aq\mathbf{I}\mathbf{J} + bp\mathbf{J}\mathbf{I} + bq\mathbf{J}\mathbf{J} &= \mathbf{I} \\
\Rightarrow ap\mathbf{I} + aq\mathbf{J} + bp\mathbf{J} + bq\dim(\mathbf{J})\mathbf{J} &= \mathbf{I} \\
\Rightarrow (ap-1)\mathbf{I} + (aq + bp + bq\dim(\mathbf{J}))\mathbf{J} &= 0 \\
\Rightarrow p = \frac{1}{a}; \qquad q &= \frac{-b}{a(a + b\dim(\mathbf{J}))} \\
\Rightarrow (a\mathbf{I} + b\mathbf{J})^{-1} &= \frac{1}{a}\left(\mathbf{I} - \frac{b}{a + b\dim(\mathbf{J})}\mathbf{J}\right)
\end{aligned} \tag{A.6}$$

- Inverse of a block diagonal matrix: If $\mathbf{M}_1, \ldots, \mathbf{M}_n$ are square matrices, then

$$[\mathrm{diag}(\mathbf{M}_1, \ldots, \mathbf{M}_n)]^{-1} = \mathrm{diag}(\mathbf{M}_1^{-1}, \ldots, \mathbf{M}_n^{-1}) \tag{A.7}$$

- Kronecker product:

$$\mathbf{J}_{[pq]}(\mathbf{I}_{[p]} \otimes \mathbf{h}_{[q]}) = q\mathbf{J}_{[pq,p]} \tag{A.8}$$

$$(\mathbf{I}_{[p]} \otimes \mathbf{h}_{[q]}^{\mathrm{T}})\mathbf{J}_{[pq,p]} = q\mathbf{J}_{[p]} \tag{A.9}$$

$$(\mathbf{I}_{[p]} \otimes \mathbf{h}_{[q]}^{\mathrm{T}})\mathbf{h}_{[pq]} = q\mathbf{h}_{[p]} \tag{A.10}$$

$$(\mathbf{P} \otimes \mathbf{Q})(\mathbf{F} \otimes \mathbf{G}) = \mathbf{P}\mathbf{F} \otimes \mathbf{Q}\mathbf{G} \tag{A.11}$$

APPENDIX B

MATHEMATICA CODE FOR HANOI NETWORK

The following program written in *Mathematica* can be used to calculate T as described in chapter(3) and plot T *vs.* E for a linear Hanoi network with all κ_i's equal to $\kappa 0$, all τ_i's equal to $\tau 0$ and all λ_i's equal to $\lambda 0$.

$\mathbf{nprecision} = 50;$

$k = 50;$

$\epsilon = 0;$

$\tau \mathbf{0} = -1;$

$\lambda \mathbf{0} = -1;$

$w = -1;$

$u = -1;$

$\mathbf{npts} = 1000;$

$\mathbf{eemin} = -2;$

$\mathbf{eemax} = 2;$

$\mathbf{Clear}[\kappa, \tau, \lambda];$

$\kappa = \mathbf{Table}[0, \{i, 1, k\}];$

$\tau = \mathbf{Table}[0, \{i, 1, k\}];$

$\lambda = \mathbf{Table}[0, \{i, 1, k\}];$

$T[\mathbf{EE\_}]:=($

$\xi = N\left[\left(-\mathbf{EE} + I\sqrt{4 - \mathbf{EE}^2}\right)\Big/ 2, \mathbf{nprecision}\right];$

$\kappa \mathbf{0} = N[\epsilon - \mathbf{EE}, \mathbf{nprecision}];$

$\kappa[[1]] = N\left[\kappa \mathbf{0} - \frac{2\tau \mathbf{0}^2}{\kappa \mathbf{0} + \tau \mathbf{0}}, \mathbf{nprecision}\right];$

$\tau[[1]] = N\left[\lambda \mathbf{0} - \frac{2\tau \mathbf{0}^2}{\kappa \mathbf{0} + \tau \mathbf{0}}, \mathbf{nprecision}\right];$

$\lambda[[1]] = N\left[\lambda 0 + \frac{\tau 0^3}{\kappa 0^2 - \tau 0^2}, \text{nprecision}\right];$

Do[

$\kappa[[m+1]] = N\left[\kappa[[m]] - 2(\lambda[[m]] - \lambda 0) - \frac{2\tau[[m]]^2}{\kappa[[m]] + \tau 0}, \text{nprecision}\right];$

$\tau[[m+1]] = N\left[\lambda[[m]] - \frac{\tau[[m]]^2}{\kappa[[m]] + \tau 0}, \text{nprecision}\right];$

$\lambda[[m+1]] = N\left[\lambda 0 + \frac{\tau[[m]]^2 \tau 0}{\kappa[[m]]^2 - \tau 0^2}, \text{nprecision}\right]$

$, \{m, 1, k-2\}];$

$\tau[[k]] = N\left[\lambda[[k-1]] - \frac{\tau[[k-1]]^2}{\kappa[[k-1]]}, \text{nprecision}\right];$

$\kappa[[k]] = N[\kappa 0 + \lambda 0 + \tau[[k]] - 2\lambda[[k-1]] + (\kappa[[k-1]] - \kappa 0)/2, \text{nprecision}];$

$\beta = N\left[\frac{wu}{\kappa[[k]]^2 - \tau[[k]]^2}, \text{nprecision}\right];$

$\gamma = N\left[\frac{u}{w}, \text{nprecision}\right];$

$N\left[\text{Abs}\left[\frac{-2I\beta\tau[[k]]\text{Im}[\xi]}{(\xi - \kappa[[k]]\beta/\gamma)(\xi - \kappa[[k]]\beta\gamma) - \beta^2\tau[[k]]^2}\right]^2, \text{nprecision}\right]$

$);$

ListLinePlot[Table[{eemin + ((nn − 1)(eemax − eemin)/(npts − 1)),

T[eemin + ((nn − 1)(eemax − eemin)/(npts − 1))]}, {nn, npts}], PlotRange → {0, 1},

PlotMarkers → {Automatic, Large}; AxesLabel → {"E", "T"}]

APPENDIX C

MATHEMATICA CODE FOR FULLY CONNECTED BETHE LATTICE

The following programs are written in *Mathematica* for a fully connected Bethe lattice with all κ_i's equal to $\kappa 0$, all τ_i's equal to $\tau 0$ and all s_i's equal to $s0$.

C.1 Transmission Amplitude

The following program calculates T as described in chapter(4) and plot T *vs.* E.

```
ClearAll[T, k, n, ϵ, τ0, s0, w0, u, κ0, κ, τ, w, ξ, c, d];

nprecision = 30;

k = 20;

n = 2;

ϵ = 0;

τ0 = −1;

s0 = −1;

w0 = −1;

u = −1;

npts = 1000;

eemin = −2;

eemax = 2;

NN[ν_]:= ((n + 1)n^(ν−1)) ;

T[EE_]:=(

κ = Table[0, {i, 1, k}];

τ = Table[0, {i, 1, k}];

w = Table[0, {i, 1, k}];

ξ = Table[0, {i, 1, k}];
```

$$\xi 0 = N\left[\left(-\text{EE} + I\sqrt{4 - \text{EE}^2}\right)\Big/ 2, \text{nprecision}\right];$$

$$\kappa 0 = N[\epsilon - \text{EE}, \text{nprecision}];$$

$$c = N\left[\tfrac{1}{\kappa 0 - \tau 0}, \text{nprecision}\right];$$

$$d = N\left[\tfrac{-\tau 0}{\kappa 0 + (\text{NN}[k]-1)\tau 0}, \text{nprecision}\right];$$

$$\kappa[[1]] = N\left[\kappa 0 - n\text{s}0^2 c(1 + nd), \text{nprecision}\right];$$

$$\tau[[1]] = N\left[\tau 0 - n^2\text{s}0^2 cd, \text{nprecision}\right];$$

$$w[[1]] = N[-n\text{s}0\text{w}0 c(1 + \text{NN}[k]d), \text{nprecision}];$$

$$\xi[[1]] = N\left[\xi 0 - \text{NN}[k]\text{w}0^2 c(1 + \text{NN}[k]d), \text{nprecision}\right];$$

$$\text{Do}[$$

$$c = N\left[\tfrac{1}{\kappa[[m]] - \tau[[m]]}, \text{nprecision}\right];$$

$$d = N\left[\tfrac{-\tau[[m]]}{\kappa[[m]] + (\text{NN}[k-m]-1)\tau[[m]]}, \text{nprecision}\right];$$

$$\kappa[[m+1]] = N\left[\kappa 0 - n\text{s}0^2 c(1 + nd), \text{nprecision}\right];$$

$$\tau[[m+1]] = N\left[\tau 0 - n^2\text{s}0^2 cd, \text{nprecision}\right];$$

$$w[[m+1]] = N[-n\text{s}0 w[[m]] c(1 + \text{NN}[k-m]d), \text{nprecision}];$$

$$\xi[[m+1]] = N\left[\xi[[m]] - \text{NN}[k-m] w[[m]]^2 c(1 + \text{NN}[k-m]d), \text{nprecision}\right];$$

$$, \{m, 1, k-2\}];$$

$$c = N\left[\tfrac{1}{\kappa[[k-1]] - \tau[[k-1]]}, \text{nprecision}\right];$$

$$d = N\left[\tfrac{-\tau[[k-1]]}{\kappa[[k-1]] + (\text{NN}[1]-1)\tau[[k-1]]}, \text{nprecision}\right];$$

$$\kappa[[k]] = N\left[\kappa 0 - (n+1)\text{s}0^2 c(1 + (n+1)d), \text{nprecision}\right];$$

$$w[[k]] = N[-(n+1)\text{s}0 w[[k-1]] c(1 + \text{NN}[1]d), \text{nprecision}];$$

$$\xi[[k]] = N\left[\xi[[k-1]] - \text{NN}[1] w[[k-1]]^2 c(1 + \text{NN}[1]d), \text{nprecision}\right];$$

$N\left[\text{Abs}\left[\frac{2I\text{Im}[\xi 0]}{\xi[[k]]\kappa[[k]]\xi 0-u^2\xi[[k]]-w[[k]]^2\xi 0}w[[k]]u\right]^2,\text{nprecision}\right]$

);

ListLogPlot[Table[{eemin + ((nn − 1)(eemax − eemin)/(npts − 1)),

T[eemin + ((nn − 1)(eemax − eemin)/(npts − 1))]}, {nn, npts}],

PlotMarkers → {Automatic, Large}; AxesLabel → {"E", "T"}]

C.2 Wavefunctions

The following program calculates ψ_i for a specific value of E as described in chapter(4) and plots $|\psi|^2$ *vs.* i; and $\Im(\psi_i)$ *vs.* $\Re(\psi_i)$.

ClearAll[r, t, EE, k, n, ϵ, τ0, s0, w0, u, κ0, $\kappa, \tau, w, \xi, c, d, \psi$];

nprecision = 30;

k = 20;

n = 2;

ϵ = 0;

τ0 = −1;

s0 = −1;

w0 = −1;

u = −1;

EE = 1.5;

NN[ν_]:= $((n+1)n^{\nu-1})$;

κ = Table[0, {i, 1, k}];

τ = Table[0, {i, 1, k}];

$w = \mathbf{Table}[0, \{i, 1, k\}];$

$\xi = \mathbf{Table}[0, \{i, 1, k\}];$

$\psi = \mathbf{Table}[0, \{i, 1, k\}];$

$\xi 0 = N\left[\left(-\mathrm{EE} + I\sqrt{4 - \mathrm{EE}^2}\right)\Big/ 2, \mathrm{nprecision}\right];$

$\kappa 0 = N[\epsilon - \mathrm{EE}, \mathrm{nprecision}];$

$c = N\left[\frac{1}{\kappa 0 - \tau 0}, \mathrm{nprecision}\right];$

$d = N\left[\frac{-\tau 0}{\kappa 0 + (\mathrm{NN}[k] - 1)\tau 0}, \mathrm{nprecision}\right];$

$\kappa[[1]] = N\left[\kappa 0 - n\mathrm{s}0^2 c(1 + nd), \mathrm{nprecision}\right];$

$\tau[[1]] = N\left[\tau 0 - n^2\mathrm{s}0^2 cd, \mathrm{nprecision}\right];$

$w[[1]] = N[-n\mathrm{s}0\mathrm{w}0c(1 + \mathrm{NN}[k]d), \mathrm{nprecision}];$

$\xi[[1]] = N\left[\xi 0 - \mathrm{NN}[k]\mathrm{w}0^2 c(1 + \mathrm{NN}[k]d), \mathrm{nprecision}\right];$

$\mathbf{Do}[$

$c = N\left[\frac{1}{\kappa[[m]] - \tau[[m]]}, \mathrm{nprecision}\right];$

$d = N\left[\frac{-\tau[[m]]}{\kappa[[m]] + (\mathrm{NN}[k-m] - 1)\tau[[m]]}, \mathrm{nprecision}\right];$

$\kappa[[m+1]] = N\left[\kappa 0 - n\mathrm{s}0^2 c(1 + nd), \mathrm{nprecision}\right];$

$\tau[[m+1]] = N\left[\tau 0 - n^2\mathrm{s}0^2 cd, \mathrm{nprecision}\right];$

$w[[m+1]] = N[-n\mathrm{s}0w[[m]]c(1 + \mathrm{NN}[k-m]d), \mathrm{nprecision}];$

$\xi[[m+1]] = N\left[\xi[[m]] - \mathrm{NN}[k-m]w[[m]]^2 c(1 + \mathrm{NN}[k-m]d), \mathrm{nprecision}\right];$

$, \{m, 1, k-2\}];$

$c = N\left[\frac{1}{\kappa[[k-1]] - \tau[[k-1]]}, \mathrm{nprecision}\right];$

$d = N\left[\frac{-\tau[[k-1]]}{\kappa[[k-1]] + (\mathrm{NN}[1] - 1)\tau[[k-1]]}, \mathrm{nprecision}\right];$

$\kappa[[k]] = N\left[\kappa 0 - (n+1)\mathrm{s}0^2 c(1 + (n+1)d), \mathrm{nprecision}\right];$

$w[[k]] = N[-(n+1)\mathbf{s0}w[[k-1]]c(1+\mathbf{NN}[1]d), \mathbf{nprecision}];$

$\xi[[k]] = N\left[\xi[[k-1]] - \mathbf{NN}[1]w[[k-1]]^2 c(1+\mathbf{NN}[1]d), \mathbf{nprecision}\right];$

$\mathbf{DummyFactor} = N\left[\frac{2I\mathbf{Im}[\xi 0]}{\xi[[k]]\kappa[[k]]\xi 0 - u^2\xi[[k]] - w[[k]]^2\xi 0}, \mathbf{nprecision}\right];$

$t = N[\mathbf{DummyFactor}w[[k]]u, \mathbf{nprecision}];$

$r = N\left[-1 + \mathbf{DummyFactor}\left(\xi 0\kappa[[k]] - u^2\right), \mathbf{nprecision}\right];$

$\psi 0 = N[-\xi 0 t/u, \mathbf{nprecision}];$

$\mathbf{Do}\left[\psi[[m]] = N\left[\frac{2I\mathbf{Im}[\xi 0] - (1+r)\xi[[k-m]]}{\mathbf{NN}[m]w[[k-m]]}, \mathbf{nprecision}\right], \{m, 1, k\}\right];$

$\mathbf{ListLogPlot}\left[\mathbf{Table}\left[\{m, \mathbf{Abs}[\psi[[m]]]^2\}, \{m, 1, k\}\right], \mathbf{Joined} \rightarrow \mathbf{True}\right]$

$\mathbf{ListLinePlot}[\mathbf{Table}[\{\mathbf{Re}[\psi[[m]]], \mathbf{Im}[\psi[[m]]]\}, \{m, 1, k\}]]$